An overview of phenomenological studies

- Dark Matter and its prospect at the LHC
- Machine learning techniques for top-tagging
- Effective field theory implications at the LHC

Arnab Roy

DHEP Annual Review
TIFR, Mumbai

Dark matter

Based on **M. Guchait, AR, S. Sharma** *Phys.Rev.D* 104 (2021) 5, 055032
And **M. Guchait, AR** *Phys.Rev.D* 102 (2020) 7, 075023

WIMP, status and exclusion

Different evidences from astrophysics and cosmology → **DM exists..**

Thermal DM

$\Omega h^2 = 0.12 \pm 0.001$ → Natural for **WIMP** → strong exclusion from different experiments

(arXiv:1807.06209, PLANCK Expt.)

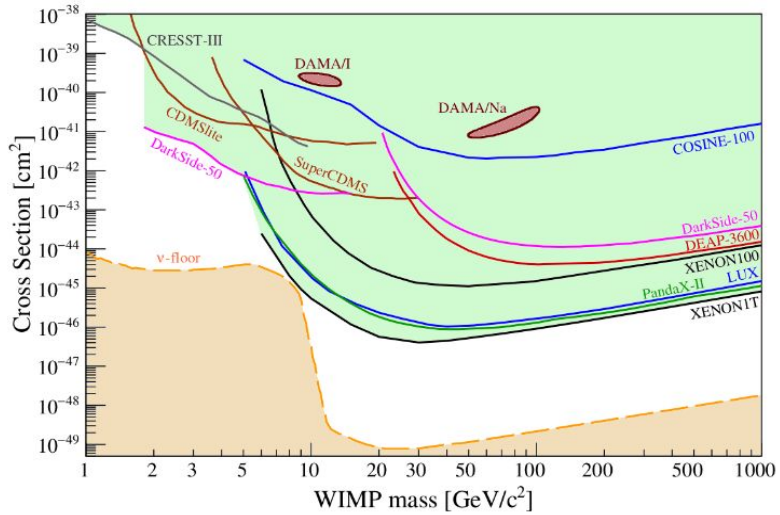

Marc Schumann, J. Phys. G46 (2019) no.10, 103003

MSSM neutralino is not a preferred option anymore

- Need **extended SUSY models (we be discussed in this talk)**

MSSM neutralino may still be a viable option

- **Highly restricted**
- **What is the current status?**
- We focus on **50-500 GeV**

Possibilities within MSSM

- Large **Higgsino** component
  - ➢ **Under-abundance** of relic density
- Large **Bino** component
  - ➢ Mostly **over-abundance**
  - ➢ But often right relic-density can be met
  - ➢ **Resonance annihilation** through Higgs, due to small Higgsino component

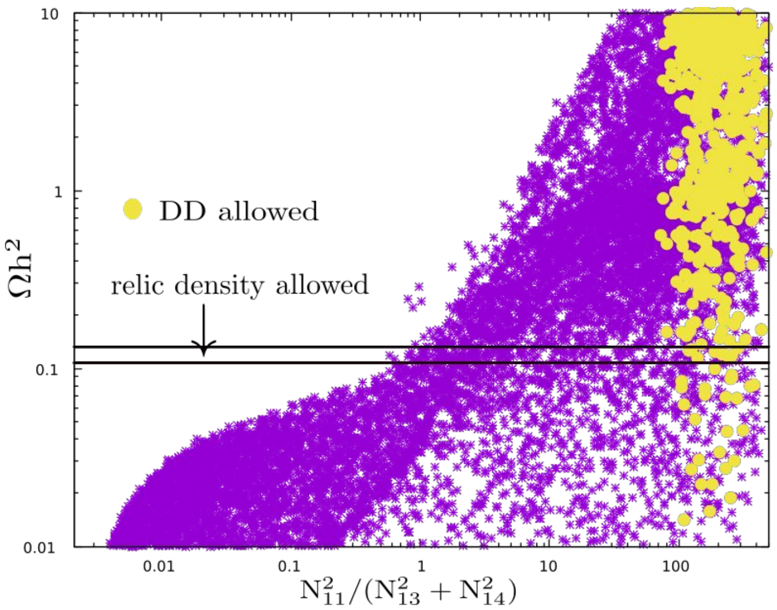

- To satisfy DD limits :

$$N_{13}^2 + N_{14}^2 \sim 1\% \text{ or less}$$

→ **Mild-tempered neutralino**

Q. Is it the only possibility?

- **Blind spots**
  - ➢ Can occur due to reduced Higgs coupling to lightest neutralino
  - ➢ Or **destructive interference between light and heavy Higgs exchange**

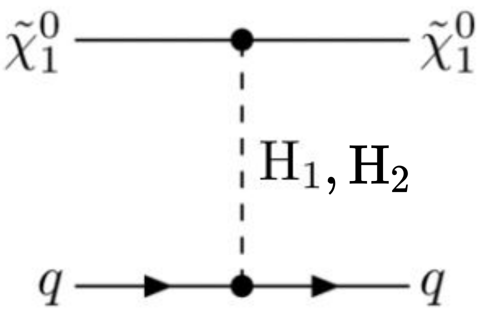

Key features

- **Bino-dominated LSP with non-negligible Higgsino component**
  - **Higgsino-like** $\tilde{\chi}^0_{2,3}$
  - The gaugino-Higgsino type $g_{h\tilde{\chi}_i\tilde{\chi}_j}$ coupling gets enhanced
- **Top-squark dominantly decays to Higgsinos**

$\boxed{\mathrm{BR}(\tilde{t}_1 \to \tilde{\chi}^0_{2,3} + t)}$ **&** $\boxed{\mathrm{BR}(\tilde{\chi}^0_{2,3} \to h + \tilde{\chi}^0_1)}$ **dominates**

➔ A **characteristic feature** of mild-tempered scenario and the allowed BS regions.

LHC implications

- **Top-squark pair production and cascade decays (This work)**

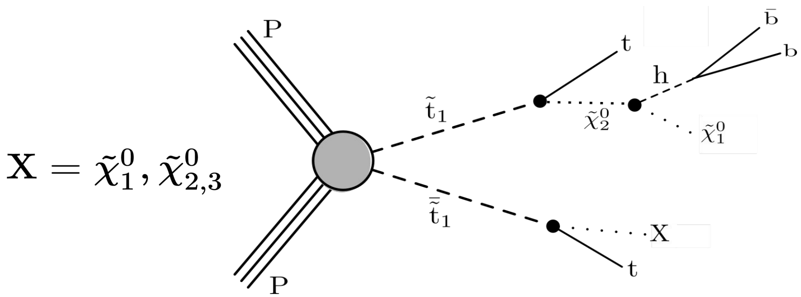

Signal

$$\boxed{h_{b\bar{b}} + \ell + \not{E}_T + (\geq 1)\ b-\mathrm{jets};\quad \ell = e, \mu}$$

Background

$$\boxed{p\ p \to t\bar{t}(1\ell),\ t\bar{t}(2\ell),\ t\bar{t}h,\ t\bar{t}Z,\ t\bar{t}b\bar{b}}$$

➔ **Resolved category** : Higgs not boosted, **b-jets are separated**

➔ **Non-resolved category**: Higgs is boosted, **b-jets are collimated**

LHC Implications (contd.)

Higgs jet reconstruction

- ❖ For the **non-resolved category**, Higgs bosons can be reconstructed as a fat jet

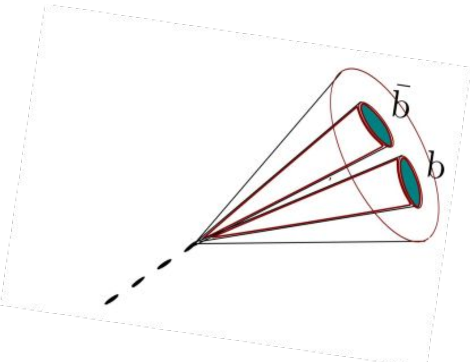

Fat-jets → MDTagger → b-matching → Higgs Jet

- In **resolved category**, pair of b-jets giving invariant mass closest to 125 GeV are identified
- If **100 GeV < m(bb) <150 GeV**, assign the resultant 4-momentum to Higgs-Jet

Other selection criteria

- **Transverse mass between lepton and MET**
- **HT: Scalar sum of pT of jets**

Signal significances (cut-based method)

- ❖ For **non-resolved category**, a significance of **1-3 σ** can be achieved at luminosity 300 fb^{-1}
- ❖ For **resolved category**, this amounts to **4-7 σ** at luminosity 300 fb^{-1}

Multivariate analysis

- ❖ Employing **MVA,** sensitivity was found to be **increased 4-5 times**

➔ **Prospects of somewhat similar analysis with strong production and cascade decay in extended SUSY model (NMSSM) is going on**, where there are extra light Higgs bosons carrying NMSSM specific signature.

Light thermal dark matter

Q. Is it possible to have a thermal DM of mass around 2-20 GeV?

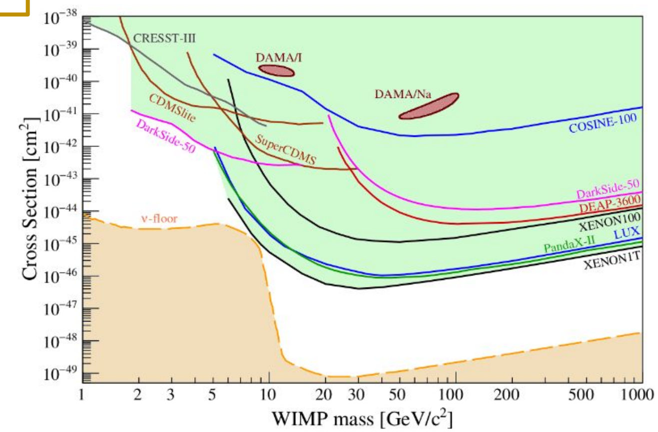

❖ **Not MSSM**

➢ Rough **Lower mass bound** on MSSM neutralino DM is **~34 GeV**

(Phys. Rev. D 95, 095018 (2017))

❖ **Any other model ?**

➢ Maybe DM is SM **singlet**, **inert to SM fermions or gauge bosons**

➢ This is natural in NMSSM when DM is **singlino-like neutralino**

➢ The **singlino-like LSP** can be **very light** in the allowed parameter space of **NMSSM**

Light Higgs bosons and neutralinos

❖ **Seven Physical Higgs States**

$$\underbrace{H_1,\ H_2,\ H_3}_{\text{3 neutral scalars}},\ \underbrace{A_1,\ A_2}_{\text{2 neutral pseudo-scalars}},\ H^{\pm}$$

Two charged Higgs

❖ Two of the **Higgs bosons (A_1, H_1) can be light**

❖ Can be still allowed by data if they are **singlet-like**

❖ **Five neutralino states**

LSP : $\boxed{\tilde{\chi}_1^0 = \mathrm{N}_{11}\widetilde{\mathrm{B}} + \mathrm{N}_{12}\widetilde{\mathrm{W}} + \mathrm{N}_{13}\widetilde{\mathrm{H}}_\mathrm{u} + \mathrm{N}_{14}\widetilde{\mathrm{H}}_\mathrm{d} + \mathrm{N}_{15}\widetilde{\mathrm{S}}}$

❖ The LSP can be below 20 GeV only if they are **Singlino-like**

$$\boxed{\mathrm{N}_{15}^2 > 95\%}$$

DM annihilation and scattering

- We need singlet-like Higgs boson states with mass :

$$\boxed{m_{A_1/H_1} \simeq 2m_{\tilde{\chi}_1^0}}$$

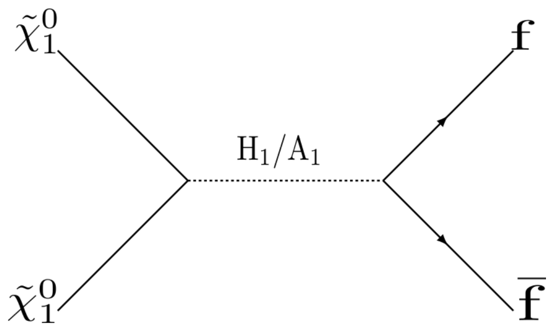

- There is **cubic coupling of singlet superfield** which makes this effective
- Corresponding **coupling parameter κ** becomes very important

- **Approximate coupling :**

$$\boxed{g_{\tilde{\chi}_1^0\tilde{\chi}_1^0 H_1} \sim \sqrt{2}S_{13}(\lambda N_{13}N_{14} - \kappa N_{15}^2) \sim -\sqrt{2}S_{13}\kappa N_{15}^2}$$

$$\boxed{g_{\tilde{\chi}_1^0\tilde{\chi}_1^0 A_1} \sim -\sqrt{2}P_{12}\kappa N_{15}^2}$$

❖ **DM - nucleon scattering**

- The **singlet-like CP-even Higgs** also takes part in DM-nucleon scattering

- The **smallness of kappa plays a important role** to keep it enough small to satisfy DD bounds

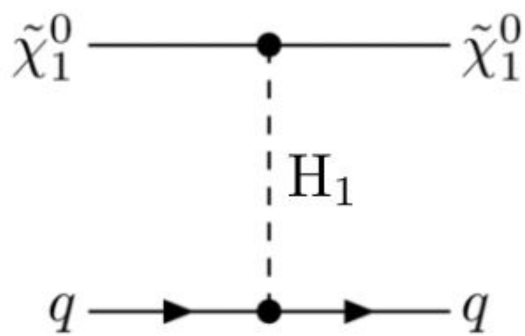

LHC Signature

- Singlino DM **indirectly** produced via production of **light singlet Higgs bosons**
- **Light singlet Higgs bosons** act as **portal** between visible and dark sector
- Decay products from these light Higgs bosons emerge as a **single fat jet, reconstructed similarly as before**

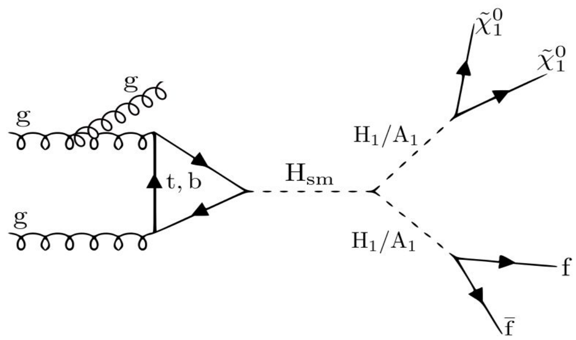

Moderate (10 GeV< m_{H1}<30 GeV) and High mass (30 GeV< m_{H1}<60 GeV)region

Signal $\boxed{J_{b\bar{b}} + \not{E}_T + \geq 1\,j}$

$$\begin{cases} \text{a) with } m_{J_{b\bar{b}}} < 30 \text{ GeV for lower mass range} \\ \text{b) with } 30 < m_{J_{b\bar{b}}} < 60 \text{ GeV for high mass range} \end{cases}$$

Dominating backgrounds $\boxed{t\bar{t},\ Wb\bar{b} + \text{jets},\ Zb\bar{b} + \text{jets}}$

Also checked $WH_{SM} + \text{jets},\ ZH_{SM} + \text{jets},\ WZ + \text{jets},\ ZZ + \text{jets}$

Low mass region (m_{H1}<10 GeV)

- **ττ decay mode** of light Higgs get enhanced
- At this very low pT, hadronic decay mode of τ suffers from large background of QCD
- We consider **leptonic decay mode of τ**

Signal $\boxed{\ell^+\ell^- + \not{E}_T + \geq 1\,j}$

Dominating backgrounds $\boxed{\text{Drell}-\text{Yan}, t\bar{t},\ W + \text{jets}, WW + \text{jets}, WZ + \text{jets}}$

Also checked Υ and J/ψ, $ZZ + \text{jets},\ ZH_{SM} + \text{jets}$

Signal Sensitivity

	BP1	BP2	BP3	BP4	BP5	BP6
$\frac{S}{\sqrt{B}}(\mathcal{L} = 300\ \text{fb}^{-1})$	6	11	14	8	7	3.5
$\frac{S}{\sqrt{B}}(\mathcal{L} = 3000\ \text{fb}^{-1})$	19	35	44	25	22	11

Low mass (BP1) **Moderate mass** (BP2–BP4) **High mass** (BP5–BP6)

ML techniques for Top-tagging

Based on **S. Bhattacharya**, M. **Guchait**, A. Vijay *Phys.Rev.D* 105 (2022) 4, 042005

Boosted top-quark and polarization

- **Top quark** is an important and interesting object to study at the LHC
- **Techniques for Tagging top jets** in **hadronic and leptonic decay** are already in literature (Godbole, Guchait, Vijay et al. 2019; Chatterjee, Godbole, Roy. 2019)
- In SM:
  - **Pair production**: top quarks are **unpolarized** (vector nature of the QCD couplings).
  - **Single top**: top quarks are **left-handed** (V −A nature of the t−b−W coupling).
- **Any change to structure of the interaction** leads to change in the **polarization of the produced top quark**.
- Hence, the **polarization of top quarks** serves as a promising window for exploring the **existence and nature of new physics**
- Measuring the **polarization of boosted top quark jets in colliders is quite challenging** – some studies have already explored different kinematic variables for this purpose. (Godbole, Guchait, Vijay et al. 2019)
- This paper describes the use of an **image-based convolutional neural network (CNN)** for **tagging boosted top-jet** and **detecting the polarization** in both hadronic and leptonic case

Jet images (example)

Hadronic Vs Leptonic

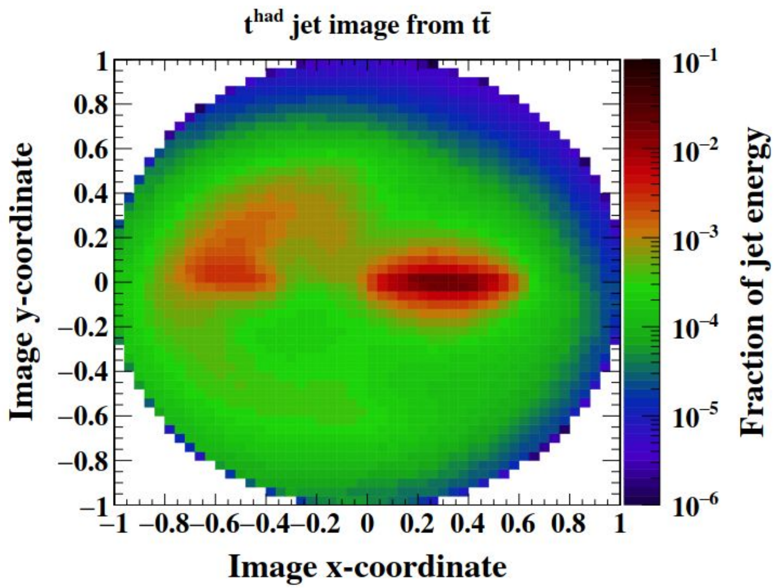

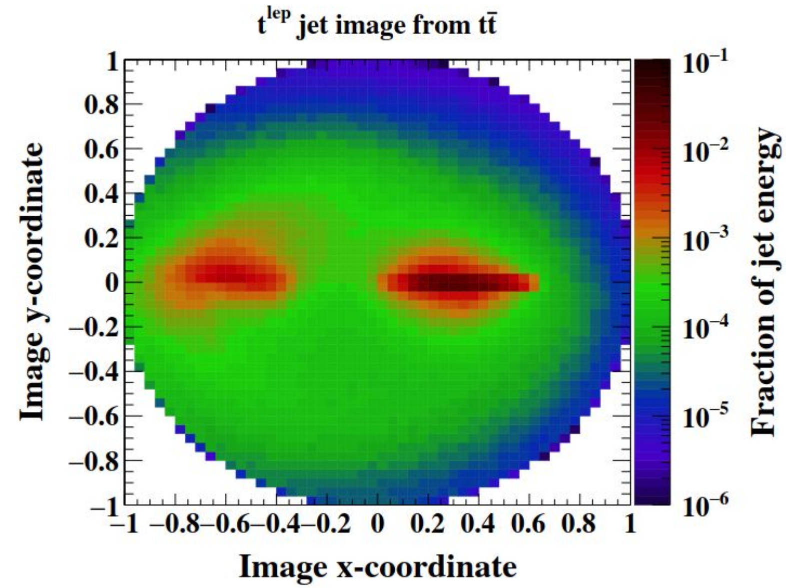

Left Vs Right

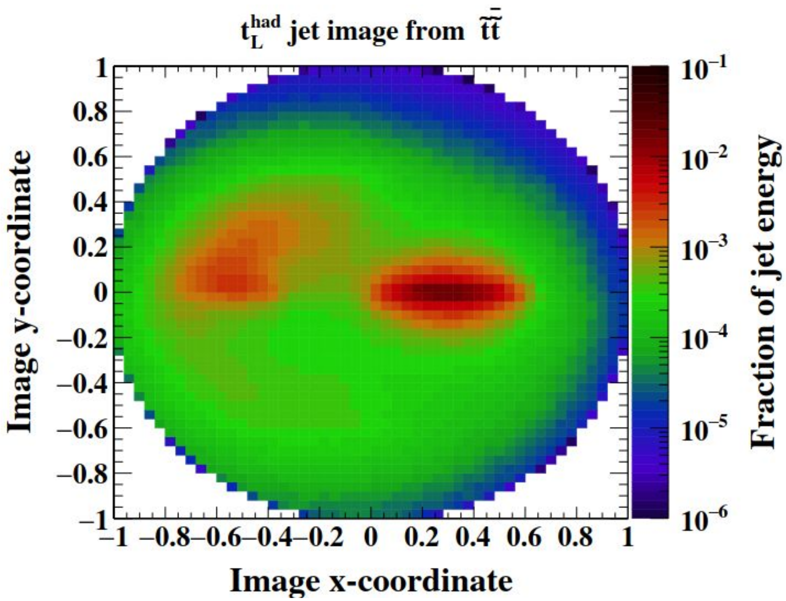

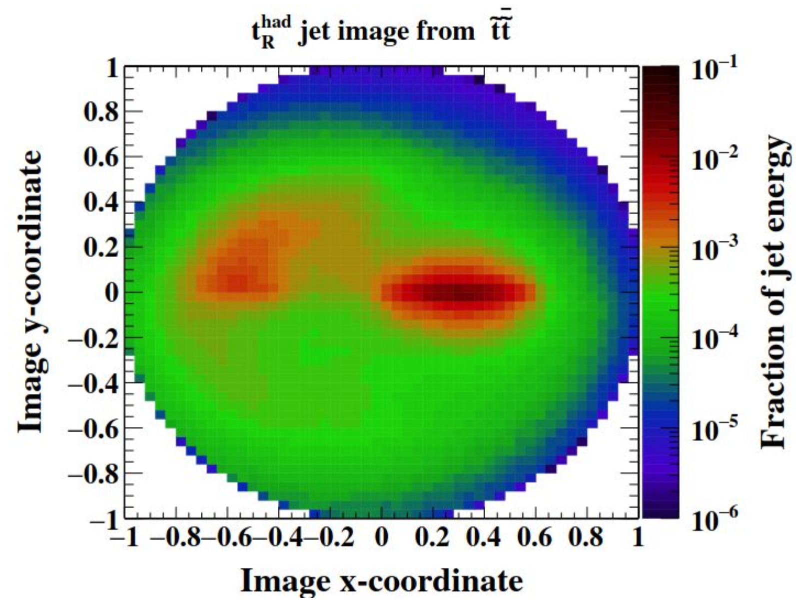

Performances of the CNN

Top-tagging

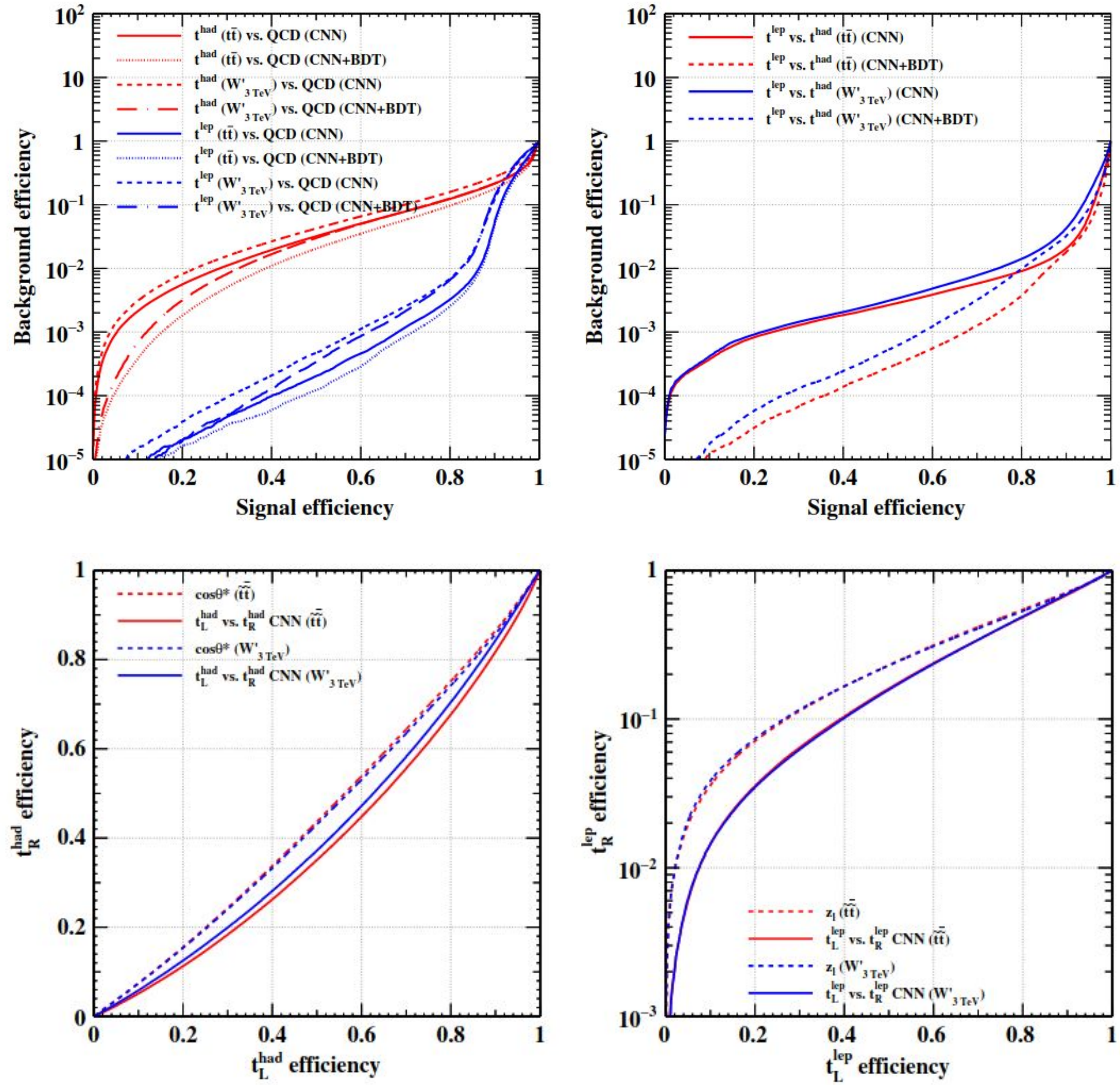

Left Vs right (hadronic top)

Left Vs right (leptonic top)

Asymmetry measurements

$$\boxed{A_v^p = \frac{N_{v>c} - N_{v<c}}{N_{v>c} + N_{v<c}}}$$

$v = \cos\theta^*, Z_l$

or CNN classifier

$$\boxed{D_v = |A_v^L - A_v^R|}$$

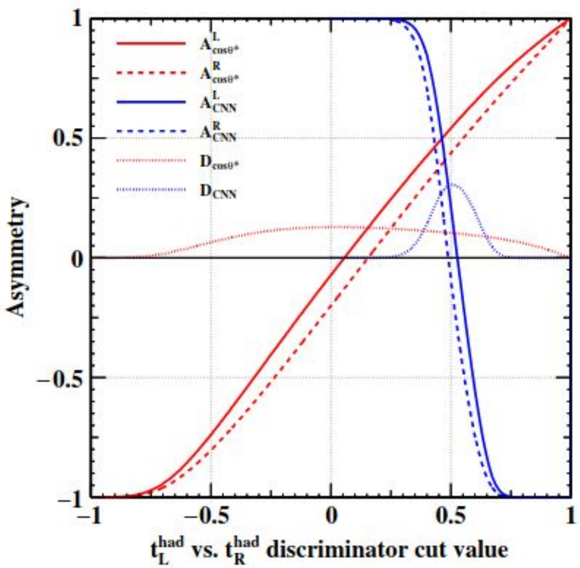

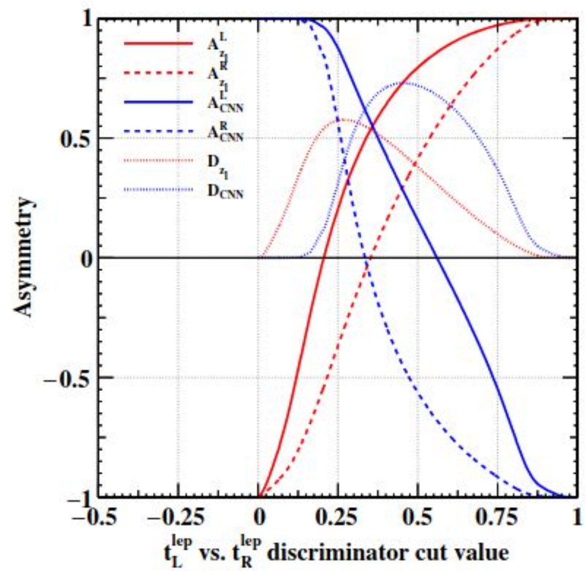

Notes

- There are **usual kinematic polarimeter** variables present in the literature
- For example **Cosθ*, Z_l** etc.

This CNN-based tagger has better sensitivity to polarization than these usual variables

Effective Field Theory

Work in progress, to be arxived soon...

SMEFT operators affecting tHq production

- The **SM has been successful**, compatible with all experimental measurements, and no evidence of light states are present till now
- This indicates **BSM physics** may reside at somewhat **higher scale**
- This motivates to interpret deviations from the dim=4 SM Lagrangian predictions in terms of an EFT:

$$\boxed{\mathcal{L}_{SMEFT} = \mathcal{L}_{SM} + \frac{1}{\Lambda^2} \sum_{i=1}^{N_{d6}} C_i^{(6)} \mathcal{O}_i^{(6)}}$$

- There can be **59 independent set of operators** in dim=6 EFT expansion
- In this work, we focus on **operators related to the tHq process** and mainly affecting top-Higgs coupling which can be a sensitive probe for new physics having close relation to EWSB
- We focus on five SMEFT operators

$$\boxed{\mathcal{O}_{t\phi}, \mathcal{O}_{\phi t}, \mathcal{O}_{pQ}^{(3)}, \mathcal{O}_{tw}, \mathcal{O}_{\phi Q}^{(-)} \equiv \mathcal{O}_{\phi Q}^{(1)} - \mathcal{O}_{\phi Q}^{(3)}}$$

Constraining ranges of the WCs

- There exists constraints from **global fits** of operators
- Some recent measurements sensitive to tHq process are not included
- We try to find a **complementary approach of constraining with a subset of data** which are most relevant and recent

Most relevant experimental data

Higgs data

$\mathrm{t\bar{t}H, tHq, tHW}$

Top data

$\mathrm{single\ top, t\bar{t}Z, t\bar{t}W, tZq, tW}$

SMEFTatNLO → **MadGraph+Madspin** → **Vary WCs to get list of cross-section** → **Polynomial Fit**

$$\sigma^{(tot)}(C) = \sigma^{(sm)} + \sum_{i=1}^{n} C_i \beta_i + \sum_{i<j}^{n} C_i C_j \gamma_{ij}$$

TMINUIT with MIGRAD → **χ2 minimization** → **Best-Fit values**

$$\mathcal{C}_{t\phi} \rightarrow -0.79^{+1.74}_{-1.6}$$
$$\mathcal{C}^{(3)}_{\phi Q} \rightarrow 1.4^{+0.6}_{-0.9}$$
$$\mathcal{C}_{\phi t} \rightarrow 0.9^{+1.1}_{-1.4}$$
$$\mathcal{C}^{(-)}_{\phi Q} \rightarrow -3.7^{+1.9}_{-0.7}$$
$$\mathcal{C}_{tw} \rightarrow -1.36^{+1.5}_{-1.0}$$

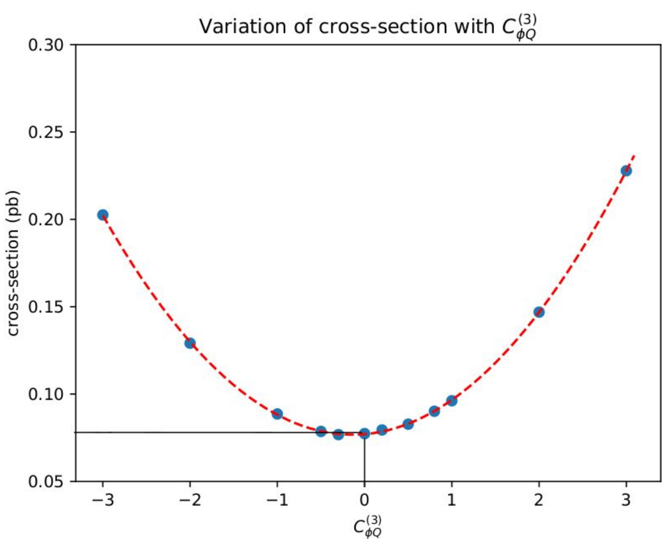

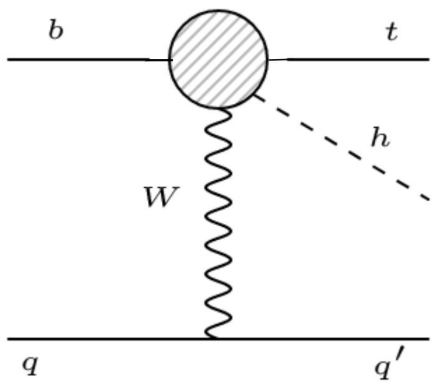

- ➔ Unlike other processes like tth, ggh etc., thq poses the **bw→ tH scattering sub amplitude**
- ➔ This results in an **energy growth** for specific operators
- ➔ We use **H→bb decay mode**
- ➔ We consider hadronic decay mode of Top-quark

Simulation

SMEFTatNLO → MadGraph → PYTHIA8 → Delphes

Event selection

- ➔ One **reconstructed Higgs Jet**
  - For boosted region, tagging **AK8 fat-jets with two b-like subjects** and **[100,150]** mass window
  - For non-boosted region, using combination of AK4 b-jets
- ➔ One **reconstructed Top Jet**
  - Using **HEPTopTagger,** in boosted region
- ➔ At least one **extra AK4 jet with pT>30 GeV**

Distributions at reconstructed level

Invariant mass of reconstructed Higgs boson Jet and top-jet

Non-boosted

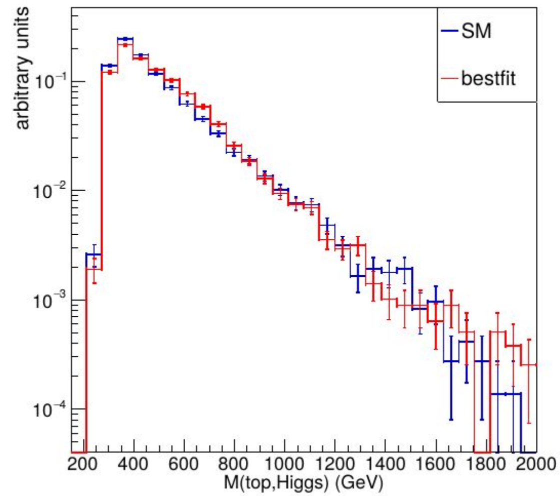

Boosted

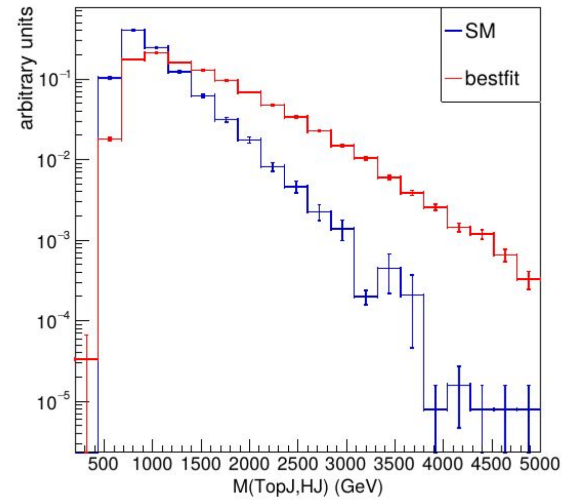

Estimation of dominating backgrounds

$\mathcal{L}$ = 300 fb^{-1}

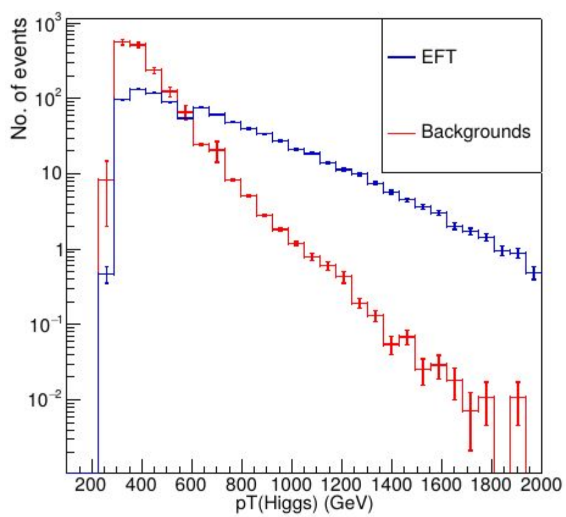

$\mathcal{L}$ = 300 fb^{-1}

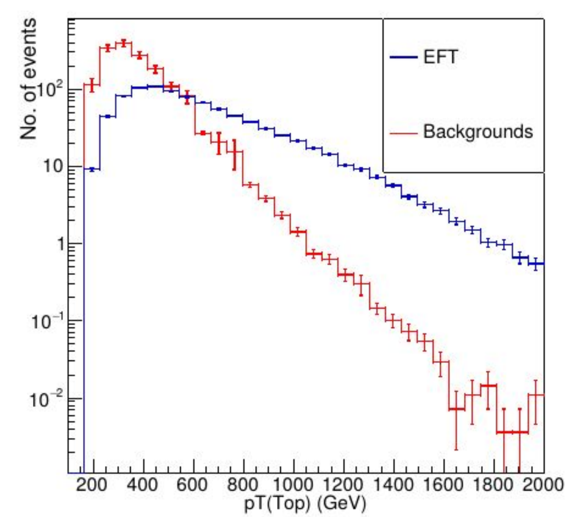

- ❖ We have considered the following backgrounds:

  $$\boxed{t\bar{t}H, t\bar{t}, t\bar{t}b\bar{b}, t\bar{t}Z, t\bar{t}W}$$

- ❖ Significant excess of events can be observed at 3000 fb^{-1} luminosity

Summary

- **Dark matter**
  - Various **possibilities of DM from GeV scale to 100 GeV scale** is explored and **sensitive search processes** were proposed.
- **Top-tagging**
  - Efficient **image-based top-tagger using CNN** is constructed having interesting capabilities to distinguish **top polarization**.
- **EFT**
  - A **set of SMEFT operators** related to tHq production is constrained and their **effects on kinematic distributions** are explored.

Future plan

- Collider prospects of **Asymmetric Dark Matter (ADM)**
- Using **ML techniques** to probe **compressed SUSY scenarios**

Back Up

Blind Spots in Dark Matter Direct Detection

Light Higgs exchange **Heavy Higgs exchange**

(Wagner et. al., Phys. Rev. D 90, 015018 (2014))

$$\sigma_p^{SI} \sim \left[\left(F_d^{(p)} + F_u^{(p)} \right) \left(m_{\tilde{\chi}_1^0} + \mu \sin 2\beta \right) \frac{1}{m_h^2} + \mu \tan\beta \cos 2\beta \left(-F_d^{(p)} + F_u^{(p)} / \tan^2\beta \right) \frac{1}{m_H^2} \right]^2$$

Decoupling limit

$$m_h << m_H$$

Intermediate m_H

$$F_d^{(p)} \sim 0.15,\ F_u^{(p)} \sim 0.14$$

reduced Higgs coupling to lightest neutralino

$$\left(m_{\tilde{\chi}_1^0} + \mu \sin 2\beta \right) = 0$$

$$\frac{M_1}{\mu} \sim -(\sin 2\beta + \tan\beta \frac{m_h^2}{2m_H^2})$$

destructive interference between light and heavy Higgs exchange

Higgsino mass μ <0, for M1>0

- ➔ **Blue**(**red**) line presents exclusion from **h,A → ττ** analysis by **CMS** (**ATLAS**) experiment
- ➔ Indicates $\mu > M_1$
- ➔ Favorably $-1.5 < \mu/M_1 < -3.5$
- ➔ Similar to mild-tempered scenario
- ➔ But often Higgsino component ~10-40% is allowed

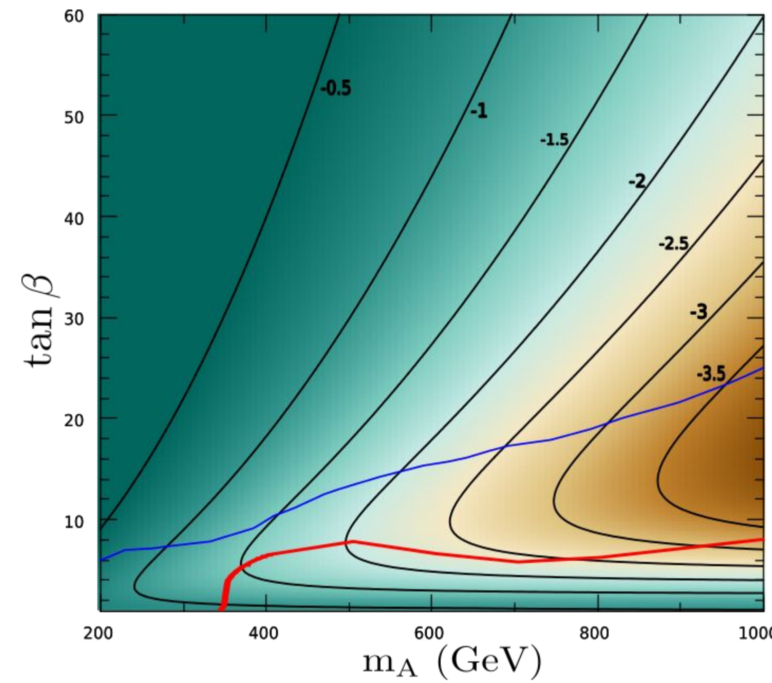

HJ reconstruction & Mass distribution

- For the **non-resolved category**, Higgs bosons can be reconstructed as a fat jet

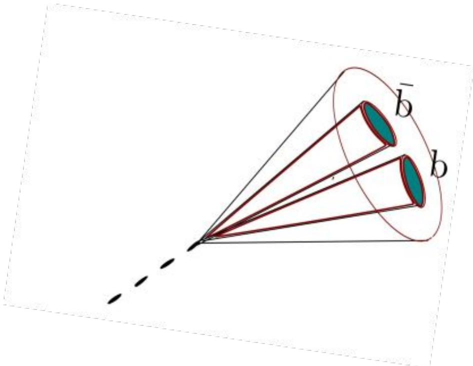

Higgs Fat Jet

- Used **MDTagger** to get tagged fat jet with two subjets
- Subjets are matched with b-quarks of the event

- In **resolved category**, pair of b-jets giving invariant mass closest to 125 GeV are identified
- If **100 GeV < m(bb) <150 GeV**, assign the resultant 4-momentum to Higgs-Jet

HJ Mass for non-resolved category

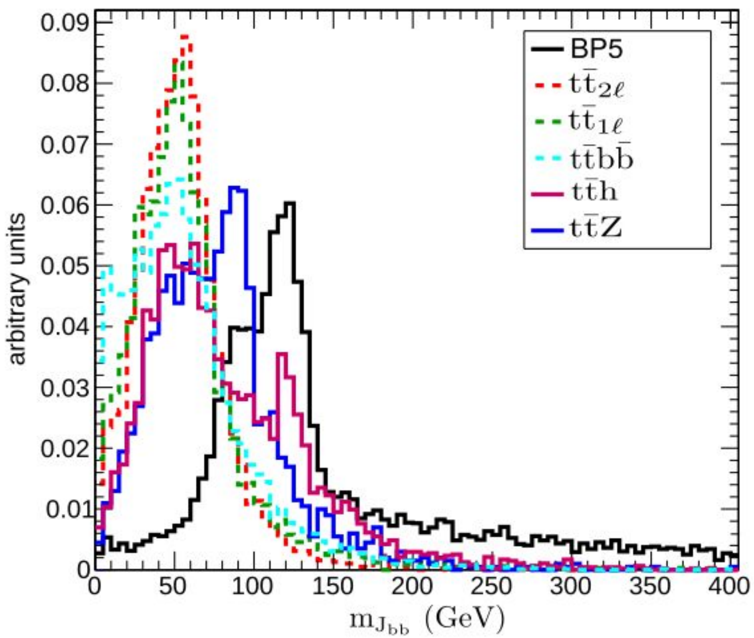

- ❖ **HJ with a specific mass requirement is a very important feature of our signal**
- ❖ Substantially different for backgrounds and signal processes
- ❖ Less effective only for tth background

$$\boxed{m_{J_{b\bar{b}}} \geq 100 \text{ GeV}}$$

Transverse Mass and HT

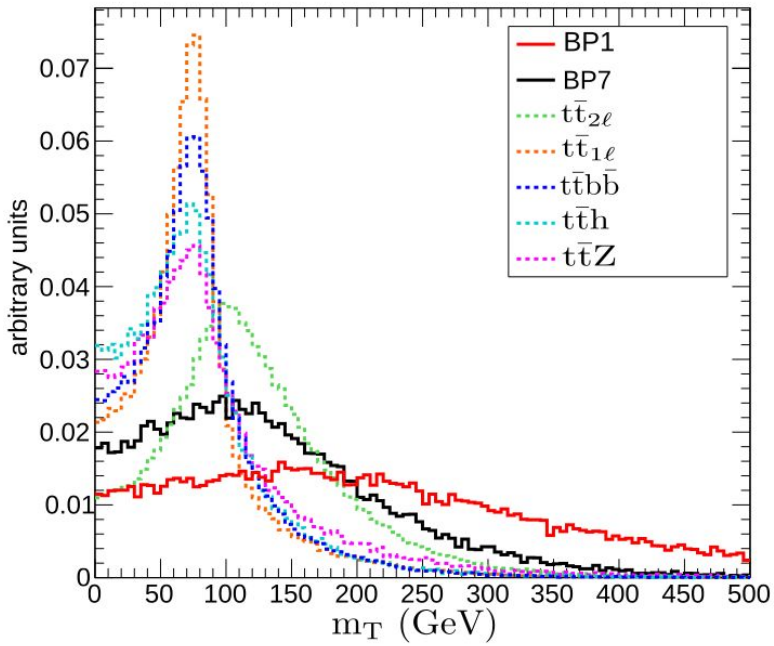

- **Transverse mass between lepton and MET**

$$m_T(\ell, \not{E}_T) = \sqrt{2 \times p_T^\ell \times \not{E}_T \times (1 - \cos\phi(\ell, \not{E}_T))}$$

$$\boxed{m_T(\ell, \not{E}_T) \geq 110 \text{ GeV}}$$

- HT : scalar sum of pT of all jets except those constitute HJ

$$\boxed{H_T \geq 500 \text{ GeV}}$$

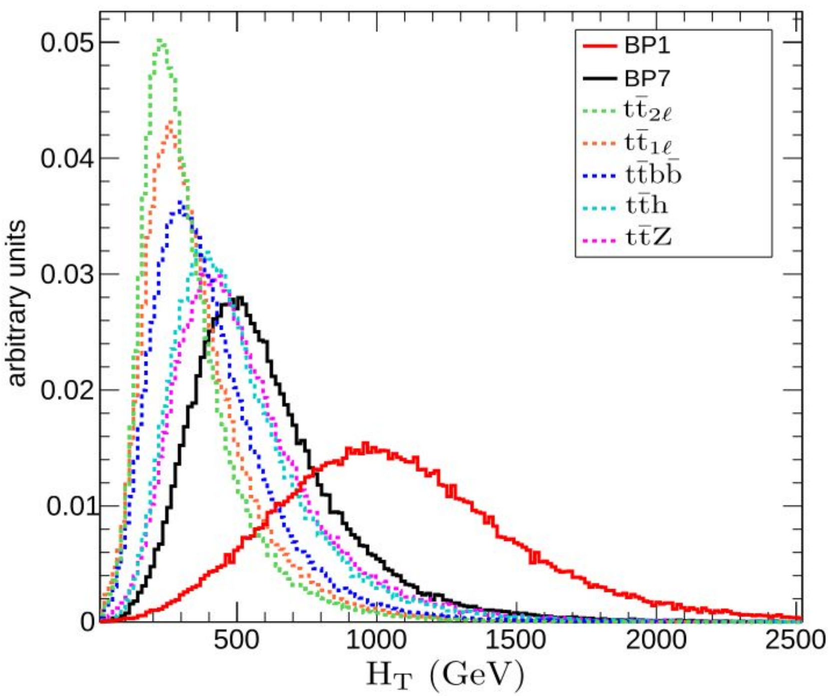

Distributions at reconstructed level

Non-boosted | **Boosted**

pT of reconstructed Higgs boson Jet

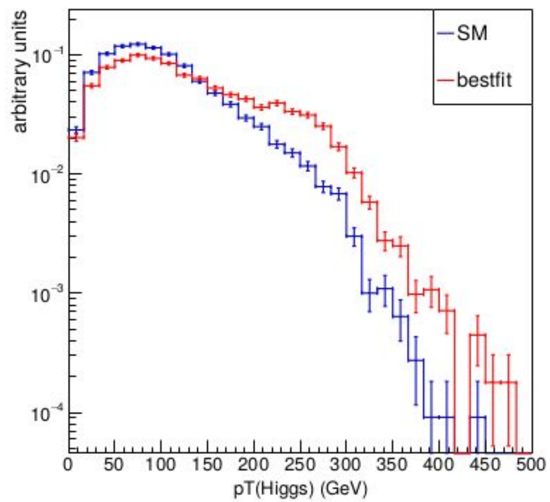

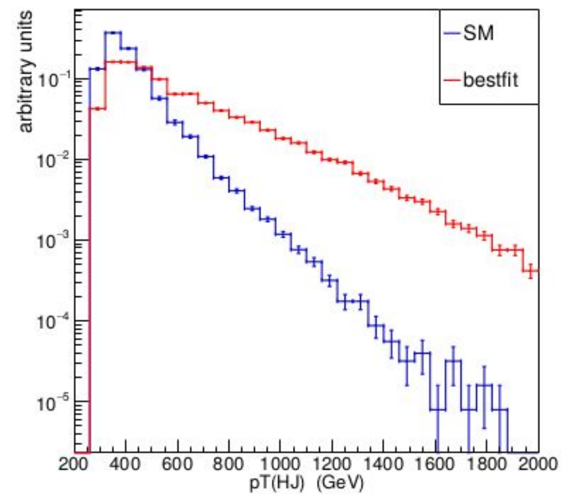

pT of reconstructed Top Jet

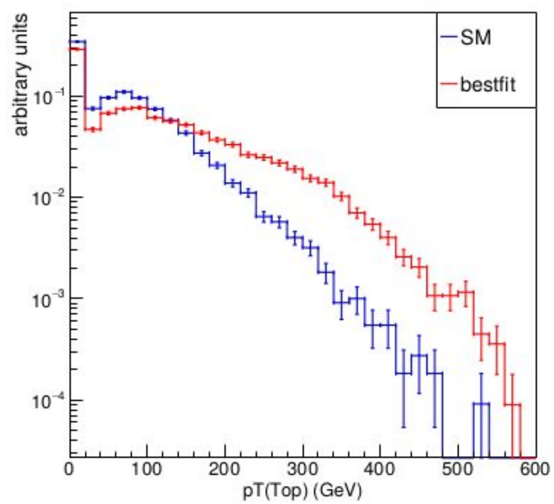

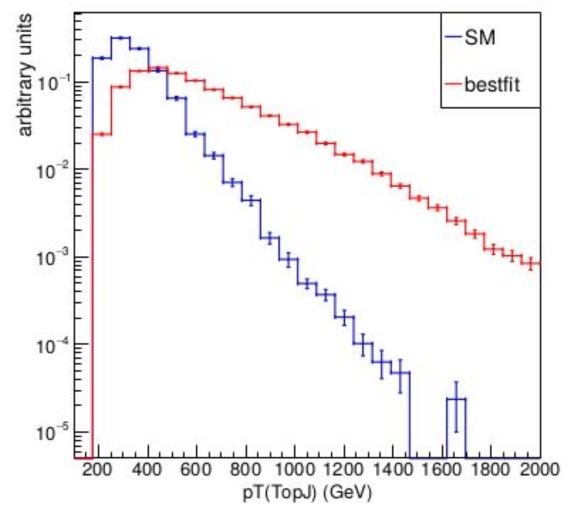

- Significant deviations are observed at the Boosted category

Angular distributions

$\Delta\phi(\text{Higgs, Top})$ $\Delta\phi(\text{Higgs, Leading Jet})$ $\Delta\phi(\text{Top, Leading Jet})$

Boosted region

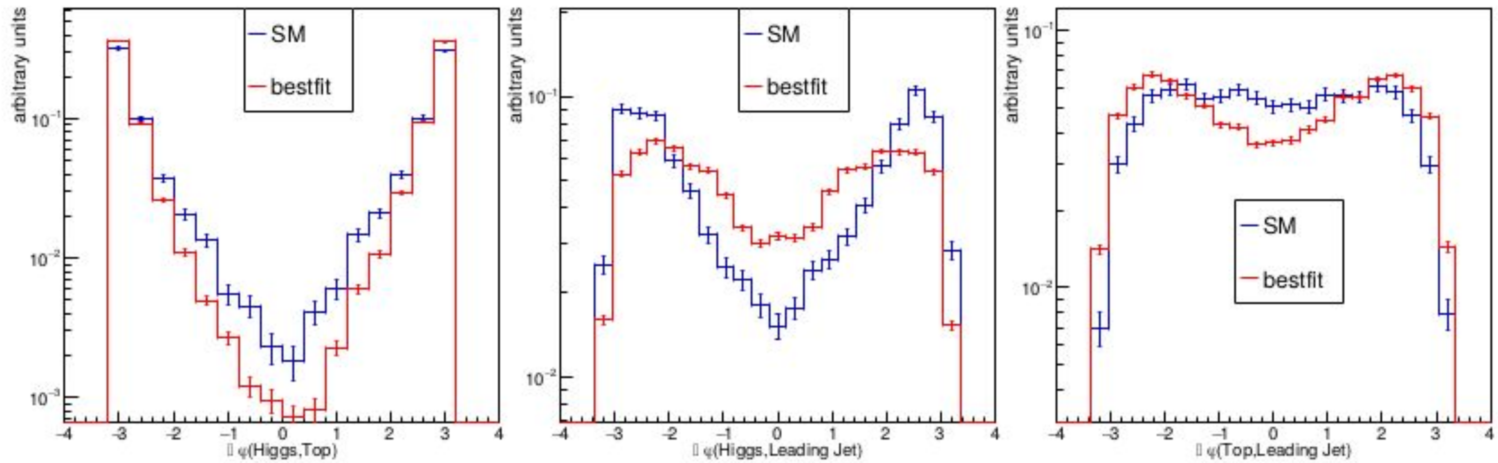

Non-boosted region

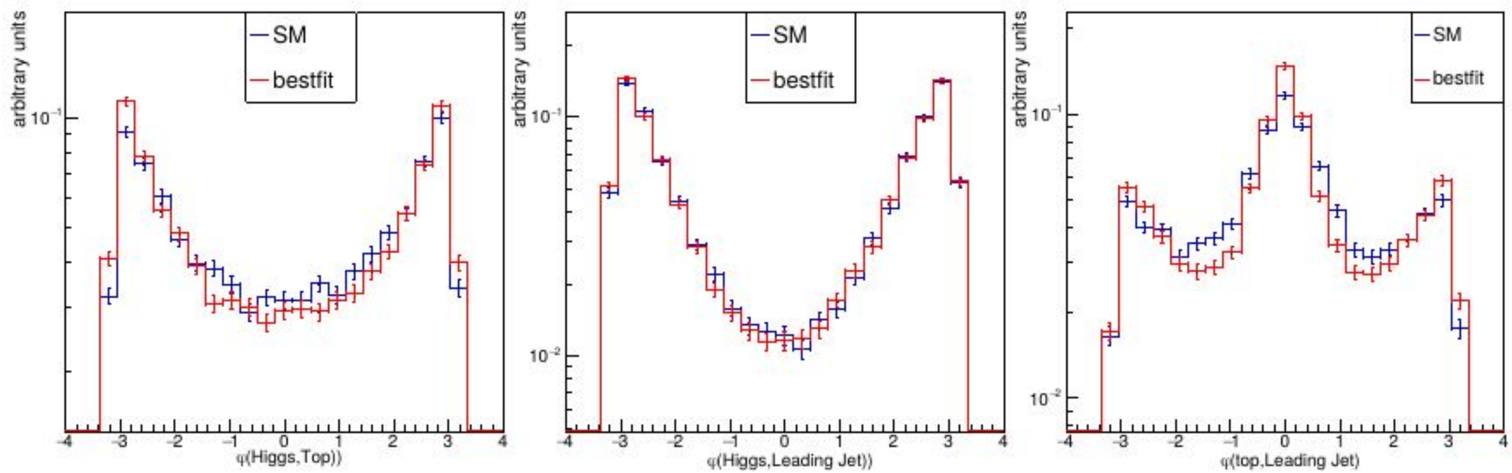

Top-quark polarization

❖ The **angular distribution (in the top rest frame)** of the top decay products is given by [Jezabek and Kuhn, 1989]:

$$\boxed{\frac{1}{\Gamma}\frac{d\Gamma}{d\cos\theta_f} = \frac{1}{2}(1 + P_0\kappa_f\cos\theta_f)}$$

- ➔ f=u,d,b,W
- ➔ P_0 = Polarization of the top quark ($-1 \leqslant P_0 \leqslant +1$)
- ➔ θ_f = Angle b/w fermion (or W) and top spin direction in the top rest frame
- ➔ κ_f = Spin analyzing power (+1, −0.3, −0.4, +0.4 for f = d, u, b, W)

❖ **For L-handed hadronic top quarks ($P_0 = -1$)**: the **b and u quarks are more likely to be aligned with the top spin** (in the top rest frame), and hence more boosted (less separated) in the lab frame.

❖ **For R-handed hadronic top quarks ($P_0 = +1$)**: the **d quark is more likely to be aligned with the top spin** (in the top rest frame), and hence more boosted in the lab frame.

❖ **Similarly for L-handed (R-handed) leptonic top quarks the b quark (lepton) will be harder**.

❖ Thus the kinematics of the decay products from L and R-handed top quarks will differ and can exploit this difference in the jet images.

Jet image formation (pre-processing)

❖ **Mass re-scaling and Lorentz boosting**

➢ Follows the technique described in 1903.02032.
1. The **jet 4-mom is rescaled such its mass is m_B**.
2. The **jet is then Lorentz boosted** to a frame in which its energy is E_B.

➢ The ratio of these two parameters ($\gamma_B = m_B / E_B$) important, and not their absolute values.

➢ We have chosen **γ_B = 2 (fairly optimal)**.

t^{had} jet image w/o pre-processing

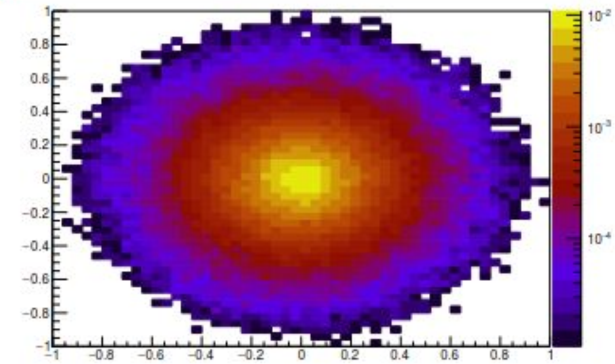

❖ **Gram-schmidt transformation**

➢ For a given jet-constituent's 4-mom pi , image coordinates are (Xi , Yi).
➢ Image size: 50×50 pixels
➢ Color axis: **Constituent energy / jet energy**

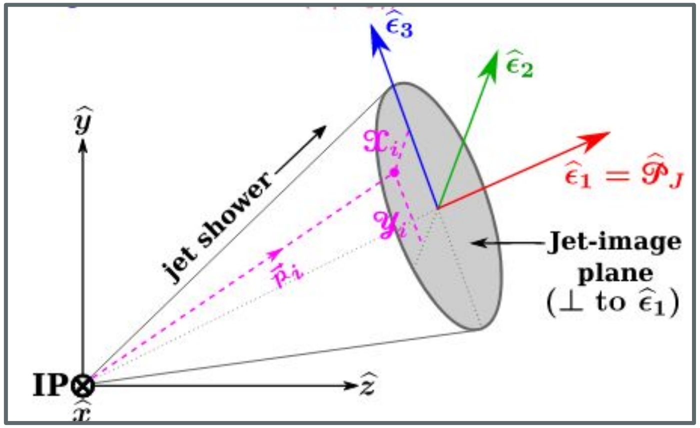

t^{had} jet image with $\gamma_B = 0$

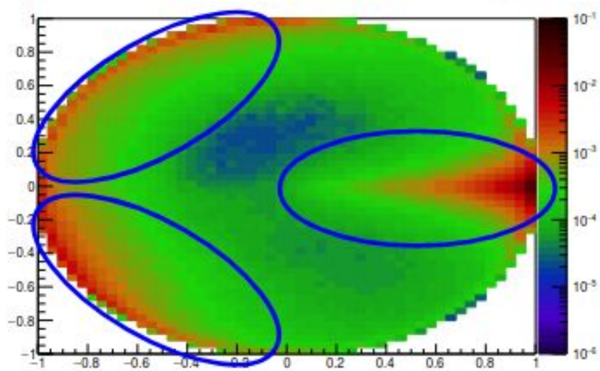

Hadronic top polarisation

- Train on hadronic $\mathrm{t_L}$ jets (from $\tilde{\mathrm{t}}_\mathrm{L}\bar{\tilde{\mathrm{t}}}_\mathrm{L}$)Vs $\mathrm{t_R}$ jets (from $\tilde{\mathrm{t}}_\mathrm{R}\bar{\tilde{\mathrm{t}}}_\mathrm{R}$)
- $\cos\theta^*$ is a kinematic variable that is shown to be quite sensitive to polarization [Godbole, Guchait et al., 2019].
  - It's the (cosine of) angle b/w the top jet (in the lab frame) and the d-like sub-jet momenta (in the top-rest frame):

$$\cos\theta^* = \frac{\vec{\mathrm{j}}_\mathrm{t} \cdot \vec{\mathrm{j}}'_\mathrm{d}}{|\vec{\mathrm{j}}_\mathrm{t}| \cdot |\vec{\mathrm{j}}'_\mathrm{d}|}$$

- The CNN outperforms $\cos\theta^*$

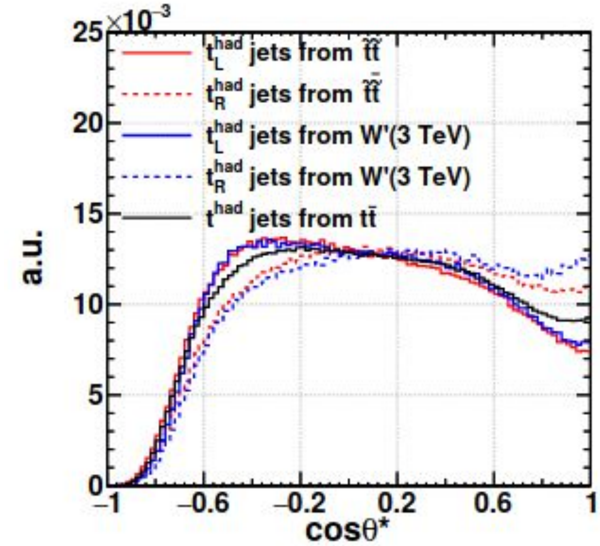

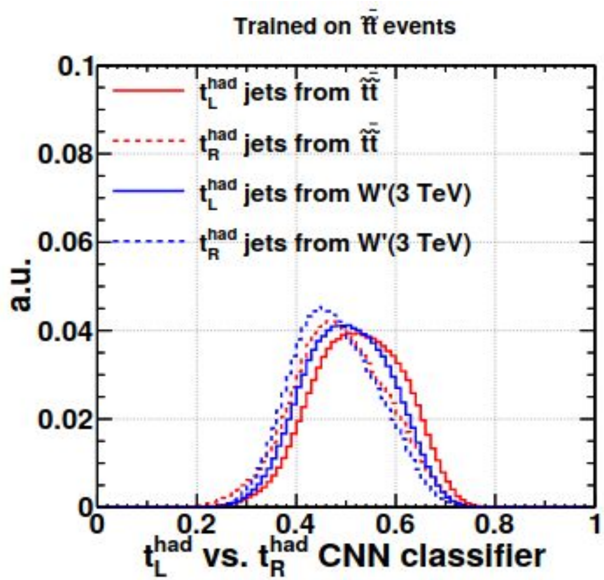

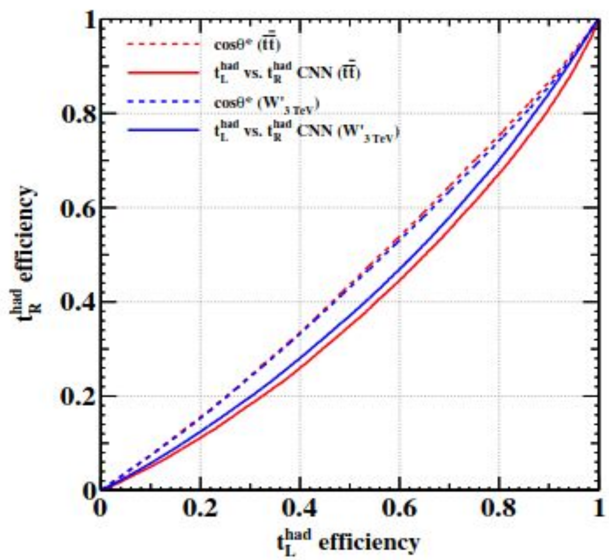

Leptonic top polarisation

- Train on leptonic t_L jets (from $\tilde{t}_L\bar{\tilde{t}}_L$)Vs t_R jets (from $\tilde{t}_R\bar{\tilde{t}}_R$)
- Z_ℓ is a kinematic variable that is shown to be quite sensitive to polarization [Godbole, Guchait et al., 2019].
  - It’s the lepton energy fraction within the top-jet.

- The CNN is independent of lepton reconstruction and ID, unlike Z_ℓ

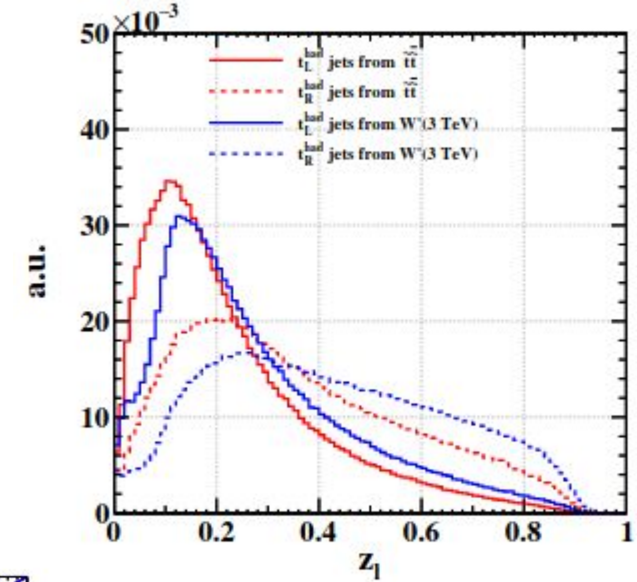

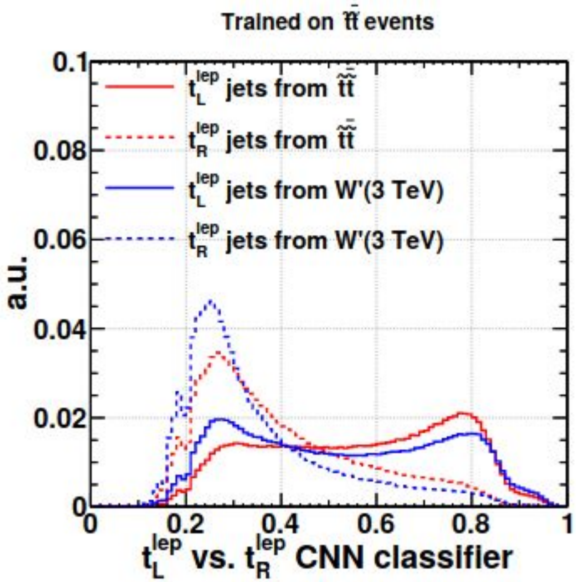

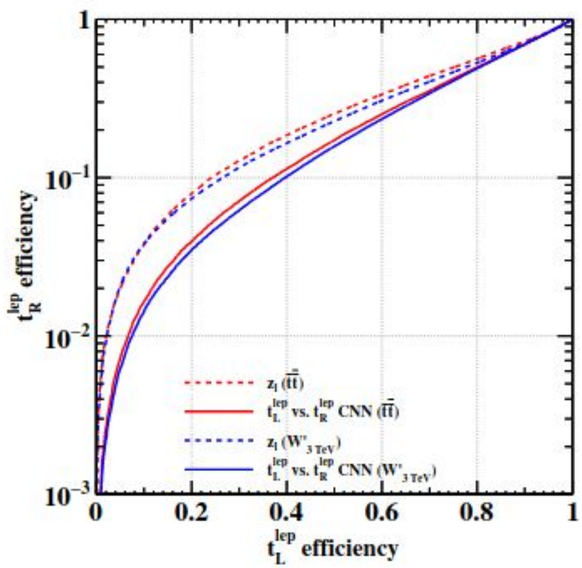

Technical details for CNN

$$\tilde{t}\bar{\tilde{t}}(\tilde{t} \to t\tilde{\chi}_1^0, m_{\tilde{t}} = 1\text{ TeV}, m_{\tilde{\chi}_1^0} = 100\text{ GeV})$$
$$W'(W' \to tb, m_{W'} = 3\text{ TeV})$$
$$t\bar{t}\text{ and QCD}(\hat{p}_T^{min} = 400\text{ GeV})$$

$$\text{MadGraph(Madspin)} \to \text{PYTHIA8} \to \text{Delphes(CMS card)}$$

- **Jet Formation**
  - **Anti-KT** jets with **R=1.5, pT > 200 GeV, |η|<2.4**
  - **Soft-drop** applied with z_cut=0.1, β =0
  - **ΔR matched** with gen-level hadronic (leptonic) top-quarks to confirm hadronic(leptonic) top-jets

The network structure

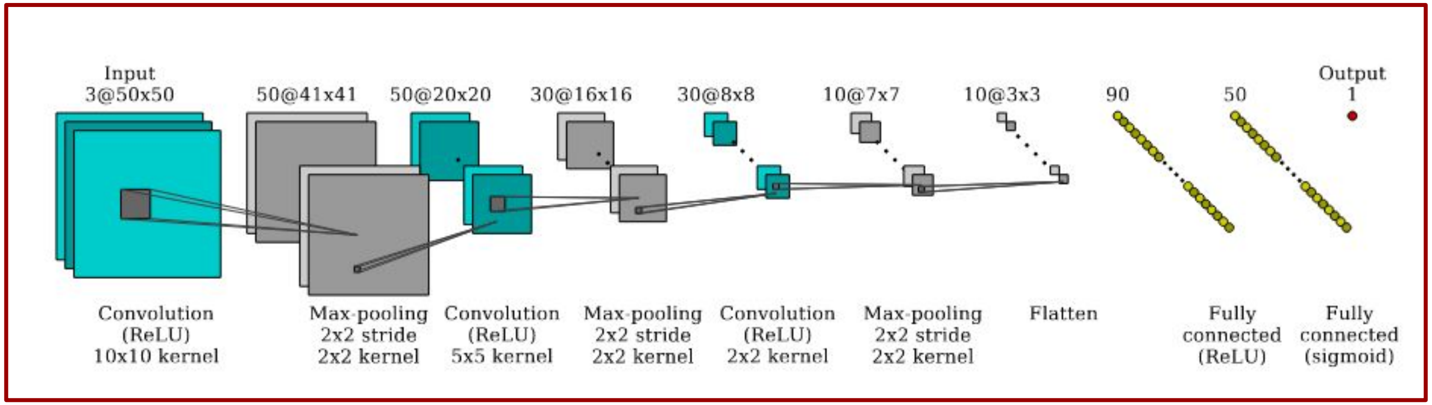

- Input has **three channels corresponding to the three jet components (tracks, photons, neutral hadrons)**.

Why CNN?

(Book: Deep Learning, Ian Goodfellow, Yoshua Bengio, Aaron Courville)

Sparse connectivity

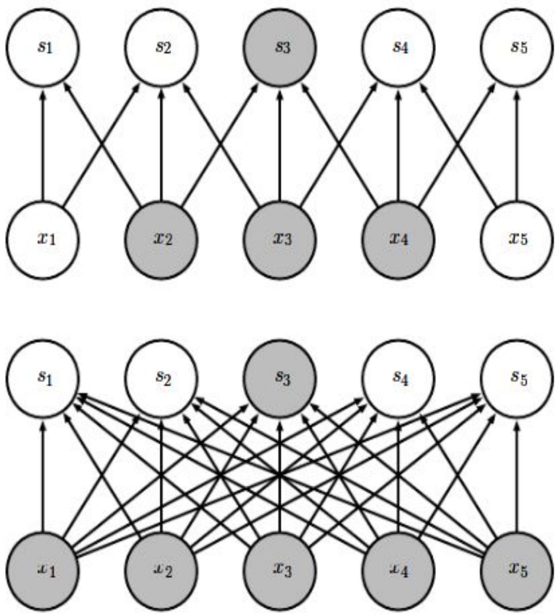

- spatial information is lost when the image is flattened (matrix to vector) into an MLP
- amount of weights rapidly becomes unmanageable for large images

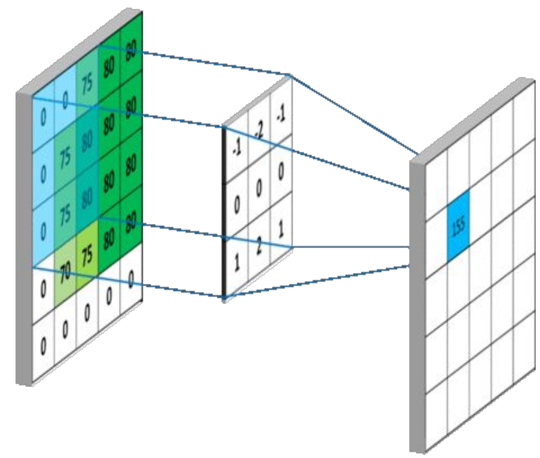

❖ each filter is panned around the entire image

❖ allows the filter to find and match patterns no matter where the pattern is located in a given image

❖ panning of filters in CNN essentially allows parameter sharing, weight sharing

Translational invariance, parameter sharing

Filters

$$\begin{bmatrix} 10 & 10 & 10 & 0 & 0 & 0 \\ 10 & 10 & 10 & 0 & 0 & 0 \\ 10 & 10 & 10 & 0 & 0 & 0 \\ 10 & 10 & 10 & 0 & 0 & 0 \\ 10 & 10 & 10 & 0 & 0 & 0 \\ 10 & 10 & 10 & 0 & 0 & 0 \end{bmatrix} * \begin{bmatrix} 1 & 0 & -1 \\ 1 & 0 & -1 \\ 1 & 0 & -1 \end{bmatrix} = \begin{bmatrix} -0 & 30 & 30 & 0 \\ 0 & 30 & 30 & 0 \\ 0 & 30 & 30 & 0 \\ 0 & 30 & 30 & 0 \end{bmatrix}$$

6 x 6   3 x 3   4 x 4

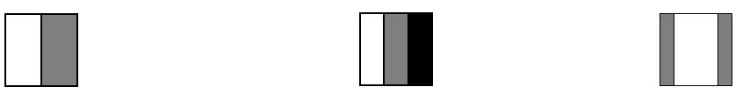

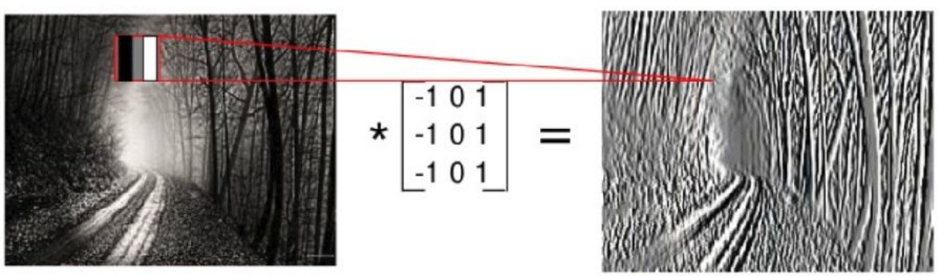

Reduction in Dimension

N x N image
F x F filter
N x N ⟶ (N-F+1) x (N-F+1)

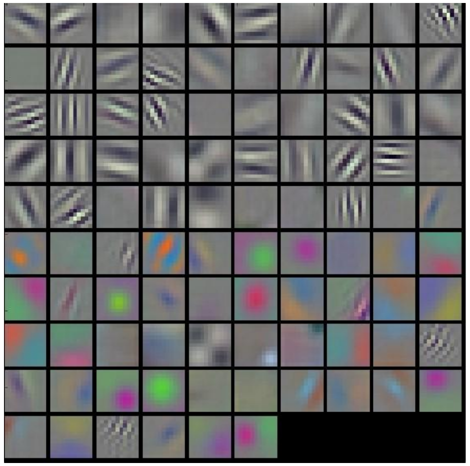

Pooling

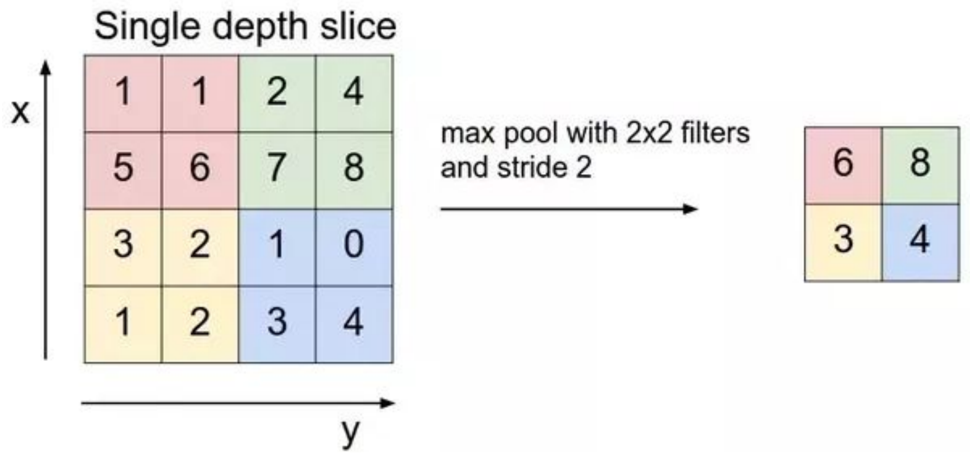

- Stride : Number of pixels/blocks to shift around

❖ **pooling** layer serves to progressively reduce the spatial size of the representation to reduce the number of parameters, memory footprint and amount of computation in the **network.**

❖ But while doing so it notes down the particular features too.

SMEFT operators affecting tHq production

- One can interpret deviations from the dim=4 SM Lagrangian predictions in terms of an EFT:

$$\boxed{\mathcal{L}_{SMEFT} = \mathcal{L}_{SM} + \frac{1}{\Lambda^2}\sum_{i=1}^{N_{d6}} C_i^{(6)} \mathcal{O}_i^{(6)}}$$

- There can be 59 independent set of operators in dim=6 EFT expansion
- In this work, we focus on **operators related to the tHq process** and mainly affecting top-Higgs coupling
- **Symmetry assumption**, to focus on top quark related operators

$$\boxed{U(3)_l \times U(3)_e \times U(2)_Q \times U(2)_u \times U(3)_d \equiv U(2)^2 \times U(3)^3}$$

- **Relevant operators**

Operator	Coefficient	Definition	Vertex	Sensitive production processes
$\mathcal{O}_{t\phi}$	$C_{t\phi}$	$(\phi^\dagger\phi - v^2/2)\bar{Q}t\tilde{\phi}$	$t\bar{t}H$	$t\bar{t}H$, tHq
$\mathcal{O}_{\phi t}$	$C_{\phi t}$	$i(\phi^\dagger \overleftrightarrow{D}_\mu \phi)\bar{t}\gamma^\mu t$	$t\bar{t}H$, $t\bar{t}V$	$t\bar{t}H$, tHq, tj, tV, $t\bar{t}Z$
$\mathcal{O}_{\phi Q}^{(1)}$	$C_{\phi Q}^{(1)}$	$i(\phi^\dagger \overleftrightarrow{D}_\mu \phi)\bar{Q}\gamma^\mu Q$	$t\bar{t}H$,Wtb	$t\bar{t}H$, tHq, tj, tV, $t\bar{t}V$
$\mathcal{O}_{pQ}^{(3)}$	$C_{\phi Q}^{(3)}$	$i(\phi^\dagger \overleftrightarrow{D}_\mu \tau_I \phi)\bar{Q}\gamma^\mu \tau^I Q$	$t\bar{t}H$,Wtb	$t\bar{t}H$, tHq, tj, tV, $t\bar{t}V$
$\mathcal{O}_{tw}$	C_{tW}	$i(\bar{Q}\sigma^{\mu\nu}\tau_I t)\tilde{\phi}W^I_{\mu\nu}$	Wtb	$t\bar{t}H$, tHq, tj, tV, $t\bar{t}V$
$\mathcal{O}_{\phi W}$	$C_{\phi W}$	$(\phi^\dagger\phi - v^2/2)W^I_{\mu\nu}W^I_{\mu\nu}$	HWW	EWPO, $t\bar{t}H$, tHq
$\mathcal{O}_{\phi D}$	$C_{\phi D}$	$(\phi^\dagger D_\mu \phi)(\phi^\dagger D^\mu \phi)$	HWW	EWPO, $t\bar{t}H$, tHq

- The operators affecting HWW vertex are found not to be much sensitive and are constrained mainly by EW precision data
- Other five are studied in this work

$$\boxed{\mathcal{O}_{t\phi}, \mathcal{O}_{\phi t}, \mathcal{O}_{pQ}^{(3)}, \mathcal{O}_{tw}, \mathcal{O}_{\phi Q}^{(-)} \equiv \mathcal{O}_{\phi Q}^{(1)} - \mathcal{O}_{\phi Q}^{(3)}}$$

Warsaw basis -I

X^3		φ^6 and $\varphi^4 D^2$		$\psi^2\varphi^3$	
Q_G	$f^{ABC} G_\mu^{A\nu} G_\nu^{B\rho} G_\rho^{C\mu}$	Q_φ	$(\varphi^\dagger\varphi)^3$	$Q_{e\varphi}$	$(\varphi^\dagger\varphi)(\bar l_p e_r \varphi)$
$Q_{\widetilde G}$	$f^{ABC} \widetilde G_\mu^{A\nu} G_\nu^{B\rho} G_\rho^{C\mu}$	$Q_{\varphi\Box}$	$(\varphi^\dagger\varphi)\Box(\varphi^\dagger\varphi)$	$Q_{u\varphi}$	$(\varphi^\dagger\varphi)(\bar q_p u_r \widetilde\varphi)$
Q_W	$\varepsilon^{IJK} W_\mu^{I\nu} W_\nu^{J\rho} W_\rho^{K\mu}$	$Q_{\varphi D}$	$\left(\varphi^\dagger D^\mu\varphi\right)^\star \left(\varphi^\dagger D_\mu\varphi\right)$	$Q_{d\varphi}$	$(\varphi^\dagger\varphi)(\bar q_p d_r \varphi)$
$Q_{\widetilde W}$	$\varepsilon^{IJK} \widetilde W_\mu^{I\nu} W_\nu^{J\rho} W_\rho^{K\mu}$				
$X^2\varphi^2$		$\psi^2 X\varphi$		$\psi^2\varphi^2 D$	
$Q_{\varphi G}$	$\varphi^\dagger\varphi\, G^A_{\mu\nu} G^{A\mu\nu}$	Q_{eW}	$(\bar l_p \sigma^{\mu\nu} e_r)\tau^I \varphi W^I_{\mu\nu}$	$Q_{\varphi l}^{(1)}$	$(\varphi^\dagger i \overleftrightarrow{D}_\mu \varphi)(\bar l_p \gamma^\mu l_r)$
$Q_{\varphi\widetilde G}$	$\varphi^\dagger\varphi\, \widetilde G^A_{\mu\nu} G^{A\mu\nu}$	Q_{eB}	$(\bar l_p \sigma^{\mu\nu} e_r)\varphi B_{\mu\nu}$	$Q_{\varphi l}^{(3)}$	$(\varphi^\dagger i \overleftrightarrow{D}^I_\mu \varphi)(\bar l_p \tau^I \gamma^\mu l_r)$
$Q_{\varphi W}$	$\varphi^\dagger\varphi\, W^I_{\mu\nu} W^{I\mu\nu}$	Q_{uG}	$(\bar q_p \sigma^{\mu\nu} T^A u_r)\widetilde\varphi\, G^A_{\mu\nu}$	$Q_{\varphi e}$	$(\varphi^\dagger i \overleftrightarrow{D}_\mu \varphi)(\bar e_p \gamma^\mu e_r)$
$Q_{\varphi\widetilde W}$	$\varphi^\dagger\varphi\, \widetilde W^I_{\mu\nu} W^{I\mu\nu}$	Q_{uW}	$(\bar q_p \sigma^{\mu\nu} u_r)\tau^I \widetilde\varphi\, W^I_{\mu\nu}$	$Q_{\varphi q}^{(1)}$	$(\varphi^\dagger i \overleftrightarrow{D}_\mu \varphi)(\bar q_p \gamma^\mu q_r)$
$Q_{\varphi B}$	$\varphi^\dagger\varphi\, B_{\mu\nu} B^{\mu\nu}$	Q_{uB}	$(\bar q_p \sigma^{\mu\nu} u_r)\widetilde\varphi\, B_{\mu\nu}$	$Q_{\varphi q}^{(3)}$	$(\varphi^\dagger i \overleftrightarrow{D}^I_\mu \varphi)(\bar q_p \tau^I \gamma^\mu q_r)$
$Q_{\varphi\widetilde B}$	$\varphi^\dagger\varphi\, \widetilde B_{\mu\nu} B^{\mu\nu}$	Q_{dG}	$(\bar q_p \sigma^{\mu\nu} T^A d_r)\varphi\, G^A_{\mu\nu}$	$Q_{\varphi u}$	$(\varphi^\dagger i \overleftrightarrow{D}_\mu \varphi)(\bar u_p \gamma^\mu u_r)$
$Q_{\varphi WB}$	$\varphi^\dagger\tau^I\varphi\, W^I_{\mu\nu} B^{\mu\nu}$	Q_{dW}	$(\bar q_p \sigma^{\mu\nu} d_r)\tau^I \varphi\, W^I_{\mu\nu}$	$Q_{\varphi d}$	$(\varphi^\dagger i \overleftrightarrow{D}_\mu \varphi)(\bar d_p \gamma^\mu d_r)$
$Q_{\varphi\widetilde WB}$	$\varphi^\dagger\tau^I\varphi\, \widetilde W^I_{\mu\nu} B^{\mu\nu}$	Q_{dB}	$(\bar q_p \sigma^{\mu\nu} d_r)\varphi\, B_{\mu\nu}$	$Q_{\varphi ud}$	$i(\widetilde\varphi^\dagger D_\mu\varphi)(\bar u_p \gamma^\mu d_r)$

Warsaw basis -II

$(\bar{L}L)(\bar{L}L)$		$(\bar{R}R)(\bar{R}R)$		$(\bar{L}L)(\bar{R}R)$	
Q_{ll}	$(\bar{l}_p\gamma_\mu l_r)(\bar{l}_s\gamma^\mu l_t)$	Q_{ee}	$(\bar{e}_p\gamma_\mu e_r)(\bar{e}_s\gamma^\mu e_t)$	Q_{le}	$(\bar{l}_p\gamma_\mu l_r)(\bar{e}_s\gamma^\mu e_t)$
$Q_{qq}^{(1)}$	$(\bar{q}_p\gamma_\mu q_r)(\bar{q}_s\gamma^\mu q_t)$	Q_{uu}	$(\bar{u}_p\gamma_\mu u_r)(\bar{u}_s\gamma^\mu u_t)$	Q_{lu}	$(\bar{l}_p\gamma_\mu l_r)(\bar{u}_s\gamma^\mu u_t)$
$Q_{qq}^{(3)}$	$(\bar{q}_p\gamma_\mu\tau^I q_r)(\bar{q}_s\gamma^\mu\tau^I q_t)$	Q_{dd}	$(\bar{d}_p\gamma_\mu d_r)(\bar{d}_s\gamma^\mu d_t)$	Q_{ld}	$(\bar{l}_p\gamma_\mu l_r)(\bar{d}_s\gamma^\mu d_t)$
$Q_{lq}^{(1)}$	$(\bar{l}_p\gamma_\mu l_r)(\bar{q}_s\gamma^\mu q_t)$	Q_{eu}	$(\bar{e}_p\gamma_\mu e_r)(\bar{u}_s\gamma^\mu u_t)$	Q_{qe}	$(\bar{q}_p\gamma_\mu q_r)(\bar{e}_s\gamma^\mu e_t)$
$Q_{lq}^{(3)}$	$(\bar{l}_p\gamma_\mu\tau^I l_r)(\bar{q}_s\gamma^\mu\tau^I q_t)$	Q_{ed}	$(\bar{e}_p\gamma_\mu e_r)(\bar{d}_s\gamma^\mu d_t)$	$Q_{qu}^{(1)}$	$(\bar{q}_p\gamma_\mu q_r)(\bar{u}_s\gamma^\mu u_t)$
		$Q_{ud}^{(1)}$	$(\bar{u}_p\gamma_\mu u_r)(\bar{d}_s\gamma^\mu d_t)$	$Q_{qu}^{(8)}$	$(\bar{q}_p\gamma_\mu T^A q_r)(\bar{u}_s\gamma^\mu T^A u_t)$
		$Q_{ud}^{(8)}$	$(\bar{u}_p\gamma_\mu T^A u_r)(\bar{d}_s\gamma^\mu T^A d_t)$	$Q_{qd}^{(1)}$	$(\bar{q}_p\gamma_\mu q_r)(\bar{d}_s\gamma^\mu d_t)$
				$Q_{qd}^{(8)}$	$(\bar{q}_p\gamma_\mu T^A q_r)(\bar{d}_s\gamma^\mu T^A d_t)$

$(\bar{L}R)(\bar{R}L)$ and $(\bar{L}R)(\bar{L}R)$		B-violating	
Q_{ledq}	$(\bar{l}_p^j e_r)(\bar{d}_s q_t^j)$	Q_{duq}	$\varepsilon^{\alpha\beta\gamma}\varepsilon_{jk}\left[(d_p^\alpha)^T C u_r^\beta\right]\left[(q_s^{\gamma j})^T C l_t^k\right]$
$Q_{quqd}^{(1)}$	$(\bar{q}_p^j u_r)\varepsilon_{jk}(\bar{q}_s^k d_t)$	Q_{qqu}	$\varepsilon^{\alpha\beta\gamma}\varepsilon_{jk}\left[(q_p^{\alpha j})^T C q_r^{\beta k}\right]\left[(u_s^\gamma)^T C e_t\right]$
$Q_{quqd}^{(8)}$	$(\bar{q}_p^j T^A u_r)\varepsilon_{jk}(\bar{q}_s^k T^A d_t)$	Q_{qqq}	$\varepsilon^{\alpha\beta\gamma}\varepsilon_{jk}\varepsilon_{mn}\left[(q_p^{\alpha j})^T C q_r^{\beta k}\right]\left[(q_s^{\gamma m})^T C l_t^n\right]$
$Q_{lequ}^{(1)}$	$(\bar{l}_p^j e_r)\varepsilon_{jk}(\bar{q}_s^k u_t)$	Q_{duu}	$\varepsilon^{\alpha\beta\gamma}\left[(d_p^\alpha)^T C u_r^\beta\right]\left[(u_s^\gamma)^T C e_t\right]$
$Q_{lequ}^{(3)}$	$(\bar{l}_p^j \sigma_{\mu\nu} e_r)\varepsilon_{jk}(\bar{q}_s^k \sigma^{\mu\nu} u_t)$		

Coefficients for ttZ

Table 7: The coefficients of various linear and quadratic terms corresponding to the fits for $t\bar{t}Z$ production cross-section.

	1	$\mathcal{C}_{t\phi}$	$\mathcal{C}_{\phi t}$	$\mathcal{C}_{\phi Q}^{(-)}$	$\mathcal{C}_{\phi Q}^{(3)}$	$\mathcal{C}_{tw}$

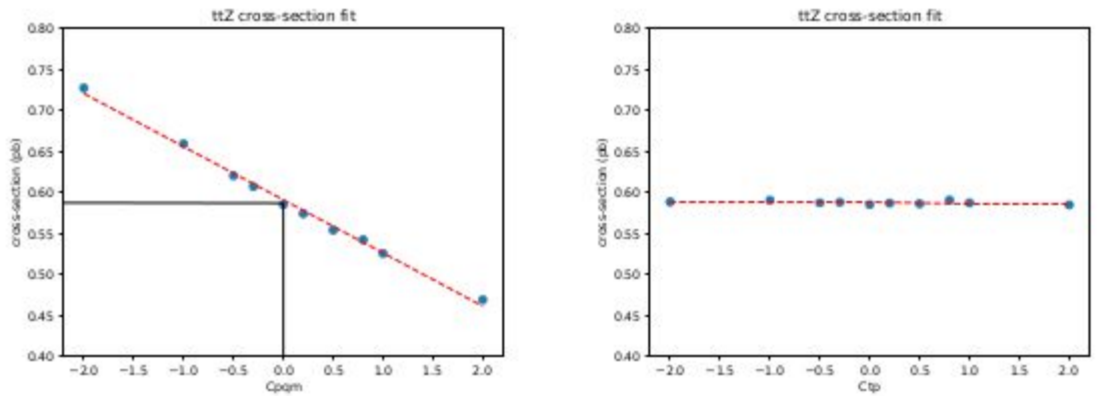

Figure 2: Variation of cross section for $t\bar{t}Z$ production with insertion of $C_{\phi Q}^{(-)}$ (left) and $C_{t\phi}$ (right), fitted with a linear polynomial.

Once expres ... ction as,

$$\chi^2(\vec{C}) = \frac{1}{N_{\mathrm{dat}}} \sum_{i,j=1}^{N_{\mathrm{dat}}} \left(\sigma_i^{\mathrm{exp}} - \sigma_i^{(\mathrm{th})}(\vec{C})\right) \mathrm{Cov}_{ij}^{-1} \left(\sigma_j^{\mathrm{exp}} - \sigma_j^{(\mathrm{th})}(\vec{C})\right). \tag{2.13}$$

Other Fits

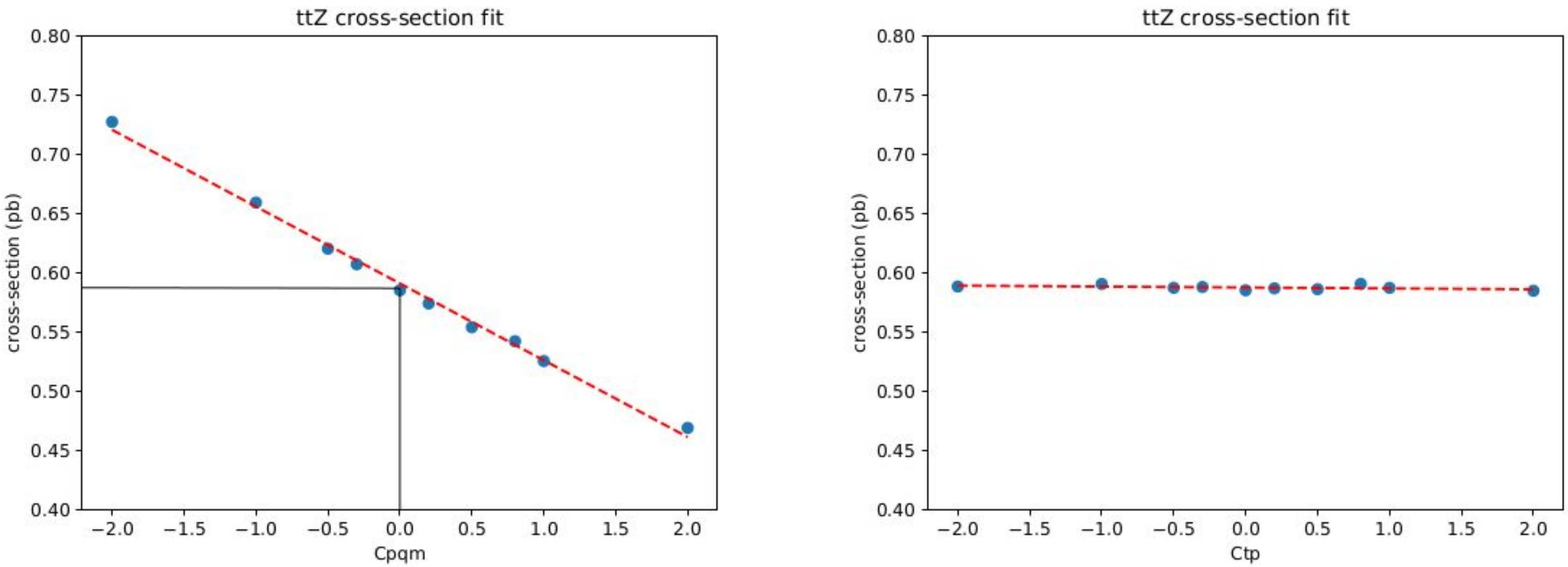

Figure 2: Variation of cross section for $t\bar{t}Z$ production with insertion of $C_{\phi Q}^{(-)}$ (left) and $C_{t\phi}$ (right), fitted with a linear polynomial.

Observable expression -I

In the framework of EFT expansion, using Eq. 2.6, we can write both the production cross-section and decay width in the following form,

$$\sigma^{(EFT)}(pp \to h)(\vec{C}) = \sigma^{(SM)} + \sum_{i=1}^{n} a_i^{\sigma} c_i + \sum_{i<j} b_{ij}^{\sigma} c_i c_j, \qquad (4.15)$$

$$\Gamma_x^{(EFT)}(\vec{C}) = \Gamma_x^{(SM)} + \sum_{i=1}^{n} a_i^{\Gamma} c_i + \sum_{i<j} b_{ij}^{\Gamma} c_i c_j, \qquad (4.16)$$

where, a_i^{σ} and b_{ij}^{σ} are polynomial coefficients for production, while a_i^{Γ} and b_{ij}^{Γ} are those for decay width. Using Eq. 2.8 4.15 and 4.16 one can write,

$$\begin{aligned}
\mu_{xx}^{(th)}(\vec{C}) = & \left(\frac{\sigma^{(SM)} + \sum_{i=1}^{N} a_i^{\sigma} c_i + \sum_{j<k} b_{jk}^{\sigma} c_j c_k}{\sigma^{SM}}\right) \times \left(\frac{\Gamma_x^{(SM)} + \sum_{l=1}^{N} a_l^{\Gamma_x} c_l + \sum_{m<n} b_{mn}^{\Gamma_x} c_m c_n}{\Gamma_x^{(SM)}}\right) \\
& \times \left(\frac{\sum_y \left(\Gamma_y^{(SM)} + \sum_{r=1}^{N} a_r^{\Gamma_y} c_r + \sum_{s<t} b_{st}^{\Gamma_y} c_s c_t\right)}{\sum_y \Gamma_z^{(SM)}}\right) \\
= & \left(1 + \sum_i \left(\frac{a_i^{\sigma}}{\sigma^{SM}}\right) c_i + \sum_{j<k} \left(\frac{b_{jk}^{\sigma}}{\sigma^{SM}}\right) c_j c_k\right) \times \left(1 + \sum_l \left(\frac{a_l^{\Gamma_x}}{\Gamma_x^{SM}}\right) c_l + \sum_{m<n} \left(\frac{b_{mn}^{\Gamma_x}}{\Gamma_x^{SM}}\right) c_m c_n\right) \\
& \times \left(\sum_y \left[\frac{\Gamma_y^{SM}}{\Gamma_{(tot)}^{SM}} + \sum_r \left(\frac{a_r^{\Gamma_y}}{\Gamma_{(tot)}^{SM}}\right) c_r + \sum_{s<t} \left(\frac{b_{st}^{\Gamma_y}}{\Gamma_{(tot)}^{SM}}\right) c_s c_t\right]\right)^{-1}
\end{aligned}$$

Observable expression - II

$$
\begin{aligned}
&= \left(1+\sum_i\left(\frac{a_i^\sigma}{\sigma^{SM}}\right)c_i+\sum_{j<k}\left(\frac{b_{jk}^\sigma}{\sigma^{SM}}\right)c_jc_k\right)\times\left(1+\sum_l\left(\frac{a_l^{\Gamma_x}}{\Gamma_x^{SM}}\right)c_l+\sum_{m<n}\left(\frac{b_{mn}^{\Gamma_x}}{\Gamma_x^{SM}}\right)c_mc_n\right)\\
&\qquad\times\left(\sum_y\left[\frac{\Gamma_y^{SM}}{\Gamma_{(tot)}^{SM}}+\sum_r\left(\frac{a_r^{\Gamma_y}}{\Gamma_{(tot)}^{SM}}\right)c_r+\sum_{s<t}\left(\frac{b_{st}^{\Gamma_y}}{\Gamma_{(tot)}^{SM}}\right)c_sc_t\right]\right)^{-1}\\
&= \left(1+\sum_i\left(\frac{a_i^\sigma}{\sigma^{SM}}\right)c_i+\sum_{j<k}\left(\frac{b_{jk}^\sigma}{\sigma^{SM}}\right)c_jc_k\right)\times\left(1+\sum_l\left(\frac{a_l^{\Gamma_x}}{\Gamma_x^{SM}}\right)c_l+\sum_{m<n}\left(\frac{b_{mn}^{\Gamma_x}}{\Gamma_x^{SM}}\right)c_mc_n\right)\\
&\qquad\times\left(1-\sum_y\left[\sum_r\left(\frac{a_r^{\Gamma_y}}{\Gamma_{(tot)}^{SM}}\right)c_r+\sum_{s<t}\left(\frac{b_{st}^{\Gamma_y}}{\Gamma_{(tot)}^{SM}}\right)c_sc_t\right]\right)
\end{aligned}
$$

$$
\begin{aligned}
&= 1+\sum_i c_i\left[\frac{a_i^\sigma}{\sigma^{SM}}+\frac{a_i^{\Gamma_x}}{\Gamma_x^{SM}}-\sum_y\left(\frac{a_i^{\Gamma_y}}{\Gamma_{(tot)}^{SM}}\right)\right]+\sum_{j<k}c_jc_k\left[\left(\frac{a_j^\sigma a_k^{\Gamma_x}}{\sigma^{SM}\Gamma_x^{SM}}\right)-\sum_y\left(\frac{a_j^\sigma a_k^{\Gamma_y}}{\sigma^{SM}\Gamma_{(tot)}^{SM}}\right)\right.\\
&\qquad\left.-\sum_y\left(\frac{a_j^{\Gamma_x}a_k^{\Gamma_y}}{\Gamma_x^{SM}\Gamma_{(tot)}^{SM}}\right)+\frac{b_{jk}^\sigma}{\sigma^{SM}}+\frac{b_{jk}^{\Gamma_x}}{\Gamma_x^{SM}}-\sum_y\left(\frac{b_{jk}^{\Gamma_y}}{\Gamma_{(tot)}^{SM}}\right)\right]\\
&= 1+\sum_i A_ic_i+\sum_{j<k}B_{jk}c_ic_j. \qquad (4.17)
\end{aligned}
$$

Bino Annihilation

- **Annihilation via t-channel light sfermions**

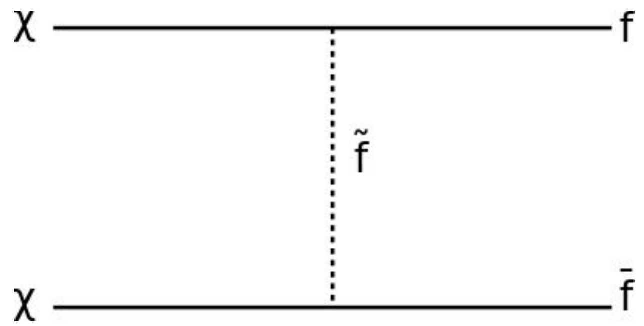

- **Coannihilation with sfermion**

❖ **ΔM should be small**
❖ **Light stau or top-squark could be helpful**

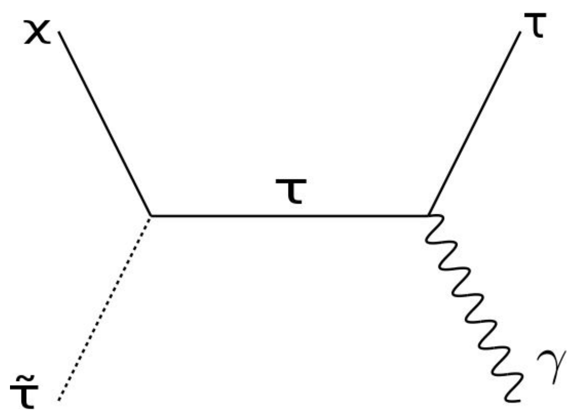

➔ None are efficient unless sfermions are light ~100 GeV or ΔM is less

➢ But presence of **non-negligible Higgsino content can help in s-channel annihilation** through Higgs or Z

Higgsino/Wino annihilation

$$\boxed{g_{Z\tilde{\chi}_1^0\tilde{\chi}_2^0} = \frac{g}{2\cos\theta_W}\left(N_{13}N_{23} - N_{14}N_{24}\right)}$$

$$\boxed{g_{W^\pm\tilde{\chi}_1^0\tilde{\chi}_1^\pm} = \frac{g\tan\theta_W}{\sqrt{2}}\left(N_{14}V_{12}^* - \sqrt{2}N_{12}V_{11}^*\right)}$$

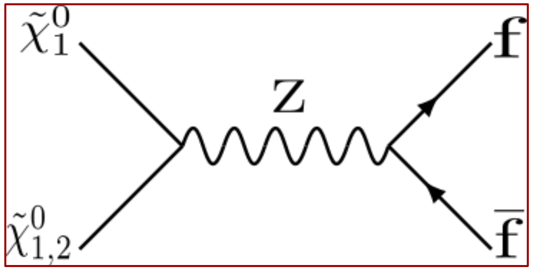

- **Annihilation into fermion pairs**

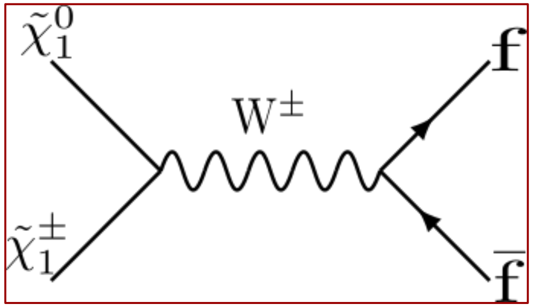

- **Coannihilation with neutralino/chargino**
  - Both are Higgsino/wino-like
  - Nearly mass degenerate

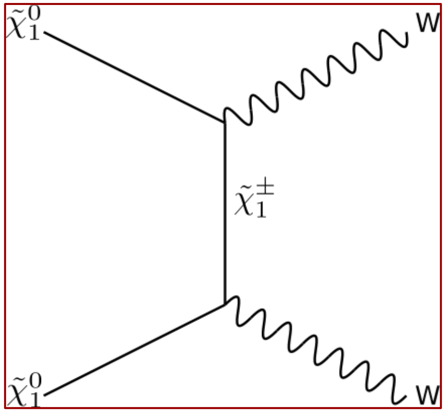

- **Annihilation into W pairs**

→ Very efficient annihilation mechanisms
→ Under-abundance of relic density

- A non-negligible bino/wino content in Higgsino enhances S-channel annihilation to fermions

Tempered neutralino

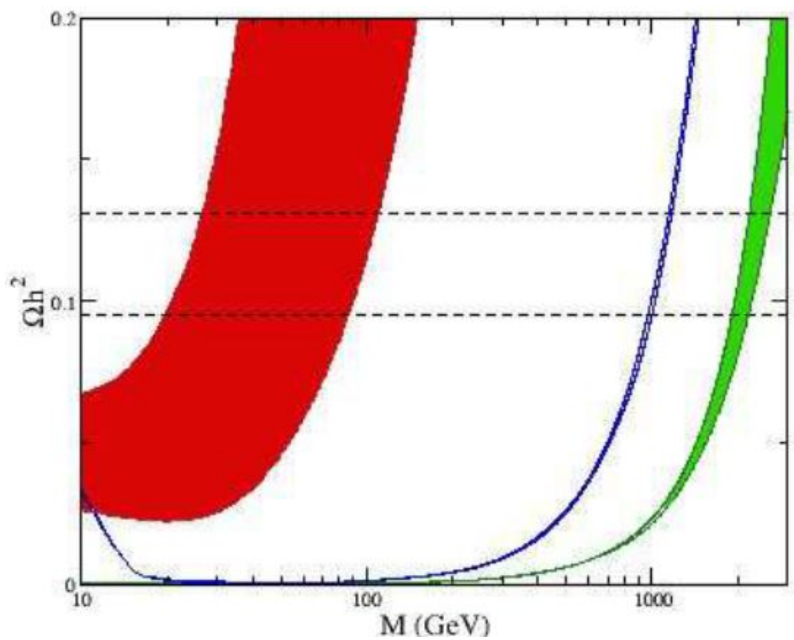

N. Arkani-Hamed et. al.
arXiv:hep-ph/0601041

Red band:
Pure bino LSP

$$0.3 < \frac{M_1}{\tilde{e}_R} < 0.9$$

Blue band:
Pure Higgsino LSP

$$1.5 < \frac{m_{\tilde{t}}}{\mu} < \infty$$

Green band:
Pure wino LSP

$$1.5 < \frac{m_{\tilde{\ell}_L}}{M_2} < \infty$$

- A pure Higgsino/Wino of mass ~100 GeV is not suitable for DM
- Unless sfermions are light, pure bino leads to overabundance of relic density.

Tempered neutralino is the solution to achieve right relic density !!

Is it compatible with limits from direct detection experiments?

Representative Benchmark Points

	BP1	BP2	BP3	BP4(**BS**)	BP5(**BS**)	BP6	BP7	BP8(**BS**)	BP9(**BS**)
M_1	60.8	58.5	274.2	334.1	296.4	204.9	352.7	238.4	248.4
M_2	2784.4	2102.4	2719.2	1438.5	1494.1	1093.6	1860.2	1561.4	1071.0
μ	655.6	793.6	984.1	-789.8	-717.5	-489.1	-610.2	-414.2	-539.9
m_A	1252.7	953.2	584.1	712.7	585.6	453.9	762.1	459.3	543.8
$\tan\beta$	7.5	6.0	6.6	6.1	6.2	5.0	5.8	6.3	6.7
M_{Q_3}	856.2	1102.2	2277.6	1024.8	1544.2	770.1	824.4	765.8	811.5
M_{t_R}	3552.0	1889	1688.8	2403.3	2061.9	2381.8	2596.2	2088.9	2634.1
$m_{\tilde{t}_1}$	954	1059	1675	1038	1475	688	804	635	765
$m_{\tilde{\chi}_3^0}$	666	802	996	800	729	494	620	424	550
$m_{\tilde{\chi}_2^0}$	666	800	994	796	725	499	618	422	545
$m_{\tilde{\chi}_1^0}$	59	58	272	335	295	207	354	238	249
$m_{\tilde{\chi}_1^\pm}$	664	799	993	795	725	495	618	420	545
m_h	125	123	123	125	124	123	123	124	125
m_H	1253	953	584	713	584	454	763	460	544
N_{11}^2	0.995	0.996	0.996	0.996	0.996	0.99	0.99	0.976	0.99
$N_{13}^2 + N_{14}^2$	0.005	0.003	0.003	0.004	0.004	0.01	0.01	0.023	0.01
Ωh^2	0.129	0.122	0.119	0.112	0.121	0.110	0.117	0.119	0.110
$\sigma_{SI}(10^{-11}$ pb$)$	5.1	5.2	10	0.009	0.02	1.9	2.4	0.69	0.002
$\sigma_{SD}(p)(10^{-7}$ pb$)$	7.2	3.2	1.6	5.2	7.5	32	21	100	26
$\sigma_{SD}(n)(10^{-7}$ pb$)$	5.7	2.5	1.3	4.1	5.8	25	12	78	20
$BR(\tilde{t}_1 \to \tilde{\chi}_1^0 + t)$	0.05	0.11	0.16	0.08	0.05	0.11	0.15	0.08	0.08
$BR(\tilde{t}_1 \to \tilde{\chi}_2^0 + t)$	0.49	0.31	0.20	0.37	0.34	0.32	0.33	0.34	0.33
$BR(\tilde{t}_1 \to \tilde{\chi}_3^0 + t)$	0.42	0.51	0.22	0.49	0.43	0.49	0.45	0.52	0.50
$BR(\tilde{\chi}_2^0 \to \tilde{\chi}_1^0 + h)$	0.70	0.73	0.70	0.73	0.72	0.85	0.83	0.78	0.75
$BR(\tilde{\chi}_3^0 \to \tilde{\chi}_1^0 + h)$	0.28	0.27	0.12	0.24	0.25	0.04	0.12	0.09	0.19

Multivariate analysis

Rank	Variable	Description
1	m_h	Mass of J_{bb}
2	HT	Scalar sum of p_T of all jets outside J_{bb}
3	$\Delta R(\not{E}_T, J_{bb})$	ΔR between $\not{E}_T$ and J_{bb}
4	$p_T(J_{bb})$	p_T of J_{bb}
5	$\not{E}_T$	Missing p_T
6	$p_T(\ell)$	p_T of leading lepton
7	$\Delta R(\not{E}_T, j)$	ΔR between $\not{E}_T$ and leading jet outside J_{bb}
8	$\Delta R(b_1, J_{bb})$	ΔR between leading b-jet (outside J_{bb}) and J_{bb}
9	Njets	Number of jets outside J_{bb}.
10	$M_T(\ell, \not{E}_T)$	Transverse Mass of leading p_T lepton and $\not{E}_T$
11	$N(\ell)$	Number of leptons
12	p_T(b-jet)	p_T of leading b-jet outside J_{bb}
13	N(b-jet)	Number of b-jets, outside J_{bb}

Non-resolved category

Rank	Variable	Description
1	$\not{E}_T$	Missing p_T
2	m_h	Mass of J_{bb}
3	$p_T(b_1)/p_T(b_2)$	pT ratio of two b-jets inside Higgs-jet.
4	$\Delta R(b_1, b_2)$	ΔR between two b-jets inside Higgs-jet.
5	$\Delta R(\not{E}_T, j)$	ΔR between $\not{E}_T$ and leading jet
6	HT	Scalar sum of p_T of all jets outside J_{bb}
7	$\Delta R(\not{E}_T, J_{bb})$	ΔR between $\not{E}_T$ and J_{bb}
8	$\Delta R(b_1, J_{bb})$	ΔR between leading b-jet (outside J_{bb}) and J_{bb}
9	Njets	Number of outside J_{bb}.
10	$p_T(\ell)$	p_T of leading lepton
11	$M_T(\ell, \not{E}_T)$	Transverse Mass of leading pT lepton and $\not{E}_T$
12	$p_T(J_{bb})$	p_T of J_{bb}
13	$N(\ell)$	Number of leptons
14	N(b-jet)	Number of b-jets, outside J_{bb}
15	p_T(b-jet)	p_T of leading b-jet outside J_{bb}

Resolved category

- ❖ Several kinematical variables are constructed
- ❖ Rankings shown are not absolute, but differs on different BPs
- ❖ overtraining tests are performed to ensure that there are no significant deviations between the performance of training and testing data
- ❖ Method used : BDTG

Flow of cuts (non-resolved category)

	BP1	BP2	BP3	BP4(**BS**)	BP5(**BS**)	$t\bar{t}(1\ell)$	$t\bar{t}(2\ell)$	$t\bar{t}h$	$t\bar{t}Z$	$t\bar{t}b\bar{b}$
Cross-secton(LO) (fb)	6	3	0.06	3	0.18	178500	36000	400	584	13700
$\not{E}_T > 200$ GeV	4.9	2.5	0.05	2.4	0.17	2695	592.5	12.6	38.8	186.7
No. of $\ell = 1$	1.5	0.75	0.02	0.7	0.05	1419	291.2	5.1	11.5	71.1
No. of $J_{bb} = 1$	0.4	0.2	0.004	0.2	0.01	33.8	12.1	1.1	0.8	10.6
$m_{J_{bb}} > 100$ GeV	0.3	0.15	0.003	0.14	0.008	11.6	2.7	0.7	0.3	2.6
No. of b-jets≥ 1	0.15	0.08	0.001	0.07	0.003	1.0	0.25	0.3	0.1	0.8
H_T >500 GeV	0.1	0.06	0.0008	0.05	0.003	0.25	0.07	0.1	0.05	0.1
$m_T(\ell, \not{E}_T) \geq$110 GeV	0.08	0.05	0.0006	0.04	0.003	0.04	0.07	0.02	0.006	0.02
$\sigma \times$ K-factor	0.12	0.07	0.001	0.056	0.004	0.06	0.1	0.024	0.008	0.04

➔ **Signal acceptance = ~1-2 %**

➔ **Background acceptance = ~0.0001%**

- **Sensitivity for points in non-Resolved category**

Blind spot

Luminosity (fb^{-1})	BP1	BP2	BP3	BP4	BP5
300	3.5	2.2	0.036	1.8	0.14
3000	11.0	6.9	0.1	5.7	0.44

Flow of cuts (resolved category)

	BP6	BP7	BP8(**BS**)	BP9(**BS**)	$t\bar{t}(1\ell)$	$t\bar{t}(2\ell)$	$t\bar{t}h$	$t\bar{t}Z$	$t\bar{t}b\bar{b}$
Cross-secton (fb)	53	19	91	34	178500	36000	400	584	13700
$\not{E}_T > 150$ GeV	31.9	12.2	46.9	25.1	8560	2100	31.3	76.5	555.6
No. of $\ell = 1$	8.7	3.3	12.7	6.8	4364	1050	12.2	23.8	204.1
No. of $J_{bb} = 1$	3.2	1.3	4.2	2.5	564.2	145.9	4.6	3.9	53.3
No. of b-jets≥ 1	2.3	1.0	2.9	1.9	49.5	11.0	3.6	1.3	35.7
H_T>500 GeV	1.3	0.6	1.6	1.2	22.3	3.6	1.7	0.6	11.8
$m_T(\ell, \not{E}_T) \geq$110 GeV	0.9	0.4	1.1	0.9	5.3	2.4	0.4	0.15	2.6
$\sigma \times$ K-factor	1.28	0.53	1.49	1.22	7.5	3.36	0.43	0.20	4.7

➔ **Signal acceptance = ~1-3 %**

➔ **Background acceptance = ~0.007%**

- **Sensitivity for points in Resolved category**

Luminosity (fb^{-1})	BP6	BP7	BP8	BP9
300	5.3	2.2	6.1	5.0
3000	16.7	6.9	19.2	15.8

Blind spot

❖ Significance are higher compared to non-resolved cases due to larger production cross sections

Separation between the two b's from Higgs

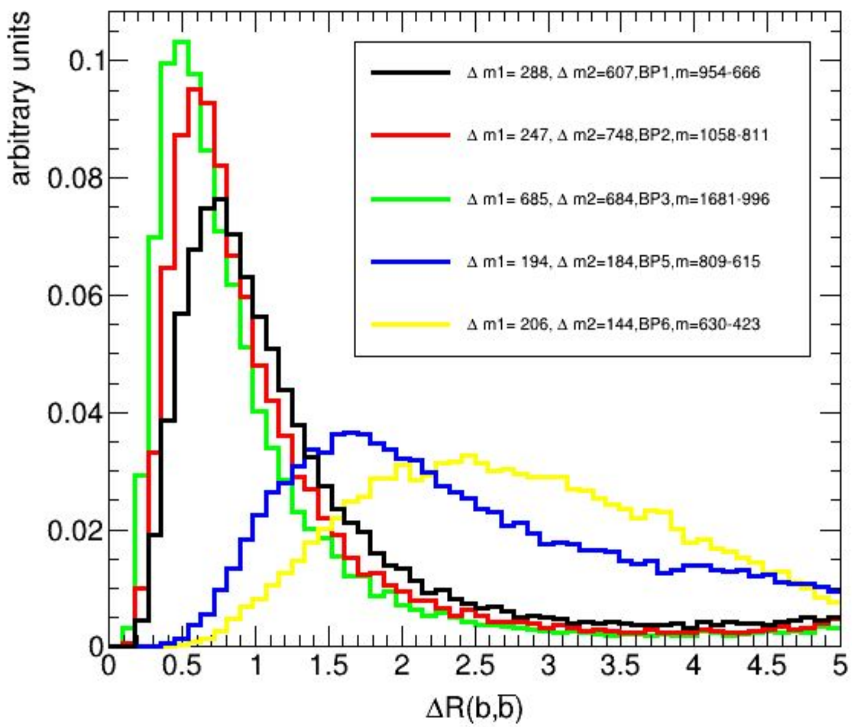

Next-to Minimal Supersymmetric Standard Model

- NMSSM Superpotential

$$\mathrm{W_{MSSM}}(\mu = 0) + \lambda \mathrm{S H_u H_d} + \frac{1}{3}\kappa \mathrm{S}^3$$

→ S gets a VEV : $v_s = \langle S \rangle$

→ We get an effective μ-term $\lambda v_s \mathrm{H_u H_d}$, with

$$\mu_{\text{eff}} = \lambda v_s \longrightarrow \text{Solves μ-problem}$$

- Also in NMSSM, SM-Higgs mass comes out more naturally than MSSM without requirement of much fine tuning

$$\mathrm{m_H^2} \simeq \mathrm{M_Z^2} \cos^2 2\beta + \lambda^2 \mathrm{v_S^2} \sin^2 2\beta + \Delta \mathrm{m_H^2}$$

Nucl. Phys. B860 (2012) 207–244

Light singlino LSP

$$
\mathrm{M_N} = \begin{pmatrix} \mathrm{M}_1 & 0 & \frac{-g_1 v s_\beta}{\sqrt{2}} & \frac{g_1 v c_\beta}{\sqrt{2}} & 0 \\ 0 & \mathrm{M}_2 & \frac{g_2 v s_\beta}{\sqrt{2}} & \frac{-g_2 v c_\beta}{\sqrt{2}} & 0 \\ \frac{-g_1 v s_\beta}{\sqrt{2}} & \frac{g_2 v s_\beta}{\sqrt{2}} & 0 & -\mu_{\mathrm{eff}} & -\lambda v c_\beta \\ \frac{g_1 v c_\beta}{\sqrt{2}} & \frac{-g_2 v c_\beta}{\sqrt{2}} & -\mu_{\mathrm{eff}} & 0 & -\lambda v s_\beta \\ 0 & 0 & -\lambda v s_\beta & -\lambda v c_\beta & 2\kappa v_s \end{pmatrix}
$$

- $\tilde{\chi}_1^0$ becomes more singlino-like, as : $|2\kappa v_s| << \mu_{\mathrm{eff}},\ \mathrm{M}_1,\ \mathrm{M}_2$
- In singlino limit : $\mathrm{M}_{\tilde{\chi}_1^0} \simeq 2\kappa v_s = 2\frac{\kappa}{\lambda}\mu_{\mathrm{eff}}$
- For very light singlino : $|\frac{\kappa}{\lambda}| \sim 10^{-2} - 10^{-1},\ \text{for}\ \mu_{\mathrm{eff}} > 100\mathrm{GeV}$

(Due to LEP limit on chargino mass)

Branching Ratios

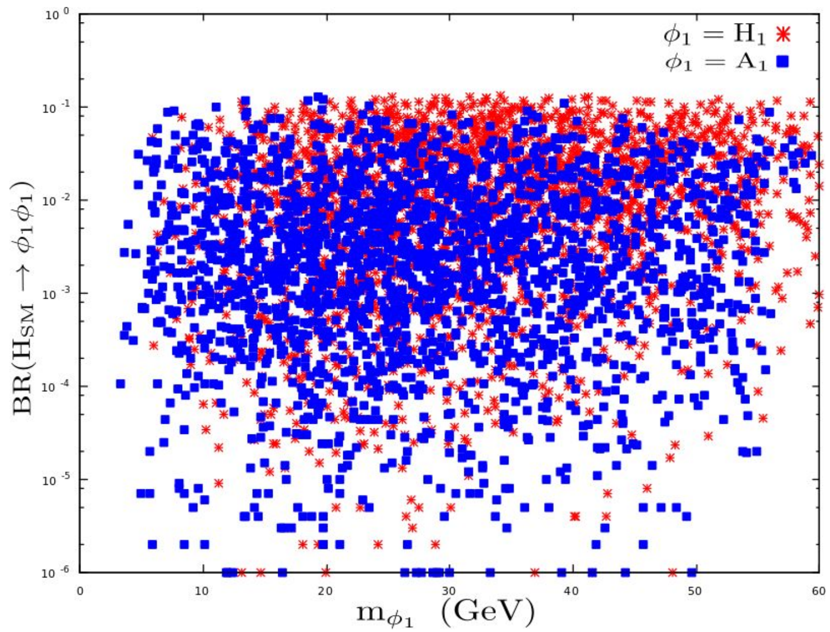

- $\mathrm{BR}(\mathrm{H_{SM}} \to \mathrm{H_1 H_1 / A_1 A_1})$ is at most 11-12% , which is well allowed by the upper limit on $\mathrm{H_{SM}} \to \mathrm{BSM}$ decay BR
- The light Higgs bosons primarily decays to $\mathrm{b\bar{b}}$ and $\tilde{\chi}_1^0 \tilde{\chi}_1^0$
- When $\mathrm{b\bar{b}}$ mode is not kinematically accessible $\tau\tau$ mode gets enhanced

Illustrative Benchmark Points

	BP1	BP2	BP3	BP4	BP5	BP6
λ	0.34195	0.17783	0.22140	0.24670	0.24980	0.29853
κ	0.00080	0.00241	-0.00564	0.00520	-0.00690	0.00438
$\tan\beta$	8.46	5.99	4.79	5.85	4.96	4.63
A_λ	3114.53	793.52	1201.50	1654.39	1968.95	1528.60
A_κ	-46.48	-29.91	36.66	-57.21	69.65	-60.15
$\mu_{\rm eff}$	340.39	150.68	232.94	290.40	378.55	364.86
m_{H_2}	123	126	126	126	123	127
m_{H_1}	43	14	28	36	44	56
m_{A_1}	8	12	24	31	47	30
$m_{\tilde{\chi}_1^0}$	3	5	10	14	20	13
Ωh^2	0.1115	0.1188	0.1188	0.1255	0.1180	0.1098
$BR(H_2 \to H_1 H_1)$	0.0001	0.06	0.01	0.11	0.08	0.07
$BR(H_2 \to A_1 A_1)$	0.10	0.004	0.06	0.001	0.02	0.01
$BR(H_1 \to b\bar{b})$	0.81	0.57	0.75	0.22	0.50	0.50
$BR(H_1 \to \tilde{\chi}_1^0 \tilde{\chi}_1^0)$	0.07	0.31	0.18	0.75	0.45	0.44
$BR(H_1 \to \tau\tau)$	0.07	0.08	0.06	0.02	0.04	0.05
$BR(A_1 \to b\bar{b})$	–	0.35	0.32	0.55	0.18	0.73
$BR(A_1 \to \tilde{\chi}_1^0 \tilde{\chi}_1^0)$	0.22	0.13	0.64	0.40	0.80	0.19
$BR(A_1 \to \tau\tau)$	0.69	0.42	0.03	0.05	0.01	0.06

Distribution of HJ mass

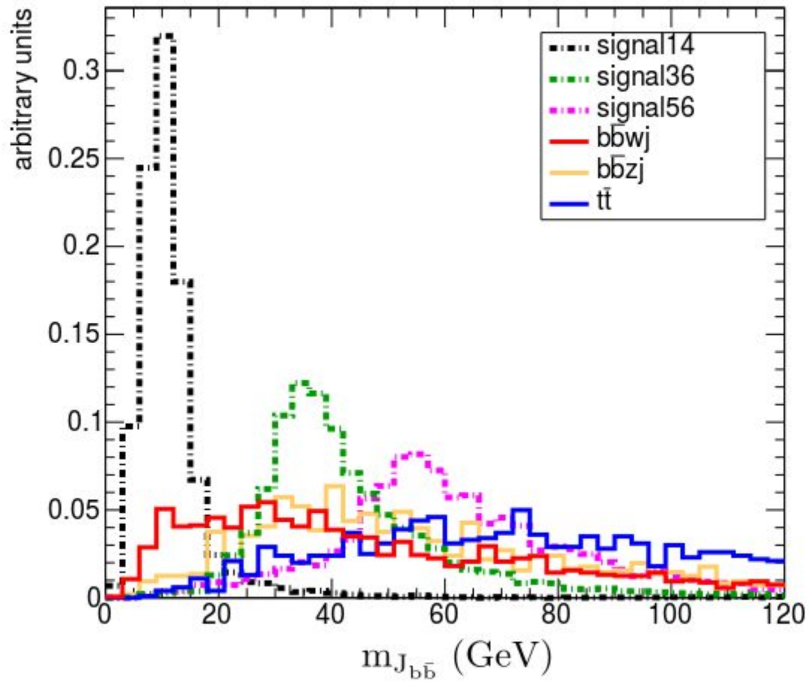

- Characteristics of HJ mass distribution are very different for backgrounds and signal processes
- Fat jet works better in lower masses than in the higher mass region
- But even in high mass region it is found to be much better than choice of two separate b-jets

Transverse Mass and R distribution

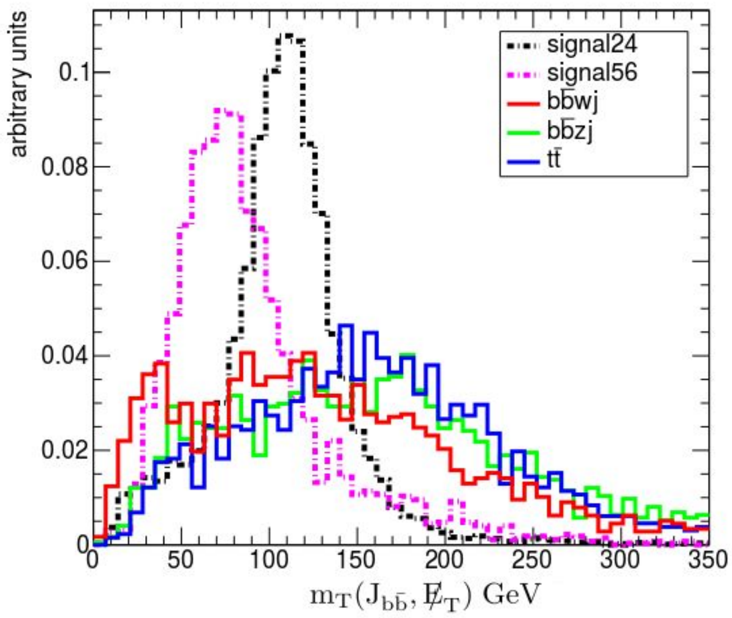

- **Transverse mass between HJ and MET**

$$m_T(J_{b\bar{b}}, \not{E}_T) = \sqrt{2 \times p_T^{J_{b\bar{b}}} \times \not{E}_T (1 - \cos\phi(J_{b\bar{b}}, \not{E}_T))}$$

→ Choose $m_T(J_{b\bar{b}}, \not{E}_T) < 140\ \mathrm{GeV}$

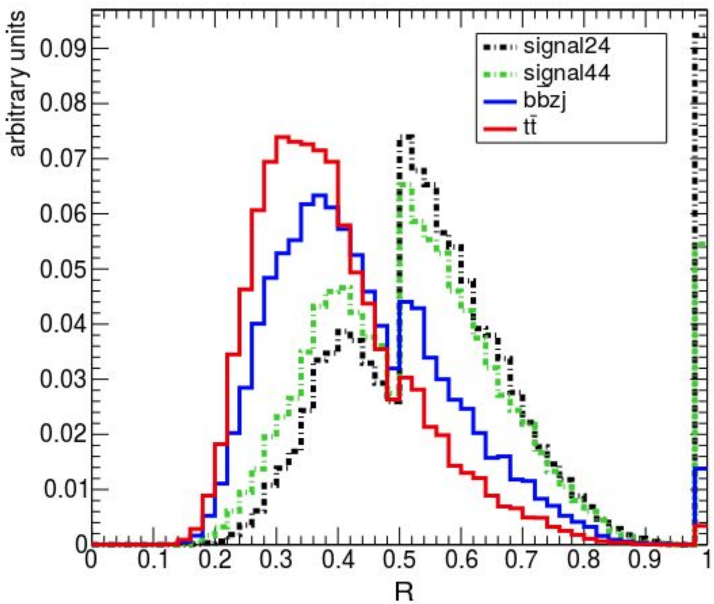

- $$R(n_j^{min}) = \frac{\sum_{i=1}^{n_j^{min}} |\vec{p}_T^{\,j_i}|}{H_T}$$

→ Very helpful for $t\bar{t}$

→ We choose R > 0.5

Flow of cuts (moderate mass region)

	BP2	BP3	$b\bar{b}Z+\text{jets}$	$b\bar{b}W+\text{jets}$	$t\bar{t}$
$\sigma(\text{pb})$	12.4	12.4	152.8	139.8	597.9
$\sigma\times\epsilon_{\text{BR}}$	0.7	0.9	152.8	139.8	597.9
lepton veto	0.6	0.8	108.5	97.6	298.2
$n_j\geq 1$	0.5	0.7	107.4	96.3	297.7
$\not{E}_T > 40.0$ GeV	0.3	0.4	32.8	24.4	109.4
No. of $J_{b\bar{b}}$ =1	0.05	0.06	1.8	3.0	4.9
$m_{J_{b\bar{b}}} < 30.0$ GeV	0.05	0.05	0.3	1.0	1.3
$m_T(J_{b\bar{b}},\not{E}_T)\leq 140$ GeV	0.04	0.04	0.2	0.8	0.9
R>0.5	0.034	0.04	0.08	0.6	0.4
$\sigma\times$ K-factor$\times\epsilon_b^2$	0.018	0.022	0.04	0.47	0.24

- **K-factors :**

$$\left.\begin{aligned} \text{signal} &\rightarrow 1.8\\ \text{bbZ}+\text{jets} &\rightarrow 1.7\\ \text{bbW}+\text{jets} &\rightarrow 2.6 \end{aligned}\right\}$$

Used MCFM

$$t\bar{t} \rightarrow 1.4$$

Melnikov, schulze
arXiv:0907.3090

- **Additional b-tagging efficiency**

$$\epsilon_b = \begin{cases} 0.66 & \text{for } t\bar{t} \\ 0.55 & \text{otherwise} \end{cases}$$

(CMS Collaboration, JINST 13 no. 05, (2018) P05011)

Flow of cuts (High mass region) and Sensitivity

	BP4	BP5	BP6	$b\bar{b}Z + \text{jets}$	$b\bar{b}W + \text{jets}$	$t\bar{t}$
$\sigma(\text{pb})$	12.4	12.4	12.4	152.8	139.8	597.9
$\sigma \times \epsilon_{\text{BR}}$	1.3	1.2	1.0	152.4	139.8	597.9
lepton veto	1.3	1.1	0.9	108.6	97.6	298.2
$n_j \geq 1$	1.2	1.0	0.9	108.0	97.3	297.8
$\not{E}_T > 35.0$ GeV	0.9	0.6	0.4	39.4	30.4	127.9
No. of $J_{b\bar{b}} = 1$	0.05	0.04	0.03	3.0	2.9	7.8
$30.0 < m_{J_{b\bar{b}}} < 60.0$ GeV	0.03	0.03	0.01	0.6	0.8	1.8
$m_T(J_{b\bar{b}}, \not{E}_T) \leq 140$ GeV	0.03	0.03	0.01	0.5	0.5	1.2
R>0.5	0.024	0.02	0.01	0.26	0.4	0.5
$\sigma \times$ K-factor $\times \epsilon_b^2$	0.013	0.011	0.0055	0.13	0.3	0.3

- **Sensitivity for both moderate and high mass region**

	BP2	BP3	BP4	BP5	BP6
$\frac{S}{\sqrt{B}}(\mathcal{L} = 300\ \text{fb}^{-1})$	11	14	8	7	3.5
$\frac{S}{\sqrt{B}}(\mathcal{L} = 3000\ \text{fb}^{-1})$	35	44	25	22	11

Flow of cuts (Low mass region) and sensitivity

	BP1	$t\bar{t}$	DY + jets	W+jets	WW+jets	WZ+jets
$\sigma \times \epsilon_{BR}$ (pb)	1.2	598	4242	5×10^4	116	51
$\not{E}_T > 30$ GeV	0.8	371.7	314.2	10771	46.8	23.7
$n_j \geq 1$	0.74	371.1	301.7	10516	45.2	23.3
N(lepton) = 2	0.005	15.2	16.5	0.2	1.1	0.4
$M_{\ell\ell} < 10$ GeV	0.0032	0.08	0.11	0.07	0.01	0.001
b-veto	0.0032	0.024	0.11	0.07	0.01	0.001
$\sigma\times$ K-factor	0.006	0.034	0.14	0.1	0.02	0.002

- **K-factors :**

$\mathrm{DY + jets} \to 1.3$ (arXiv:2001.11377)

$\mathrm{W + jets} \to 1.4$ Phys. Rev. Lett. 115 no. 6, (2015) 062002

$\mathrm{WW + jets} \to 1.8$ Phys. Rev. Lett. 113 no. 21, (2014) 212001

$\mathrm{WZ + jets} \to 2.07$ Phys. Lett. B 761 (2016) 179–183

- **signal sensitivity**

$$\boxed{\frac{S}{\sqrt{B}} = \begin{cases} 6 \ \ (\mathcal{L} = 300\ \mathrm{fb}^{-1}) \\ 19\ (\mathcal{L} = 3000\ \mathrm{fb}^{-1}) \end{cases}}$$

Sneutrino can not be DM in the MSSM

Sneutrino is the superpartner of the left-handed (LH) neutrino: is a $SU(2)_L$ doublet
(Y=1 ⟶ couples to the Z boson)